AD-A106 792 CALIFORNIA UNIV BERKELEY ELECTRONICS RESEARCH LAB F/G 12/1
ALGORITHMS FOR COMPUTING ALMOST-PERIODIC STEADY-STATE RESPONSE --ETC(U)
DEC 80 L O CHUA, A USHIDA N00014-76-C-0572
UNCLASSIFIED UCB/ERL-M80/55 NL

1 OF 1
AD A

END
DATE FILMED
11-81
DTIC

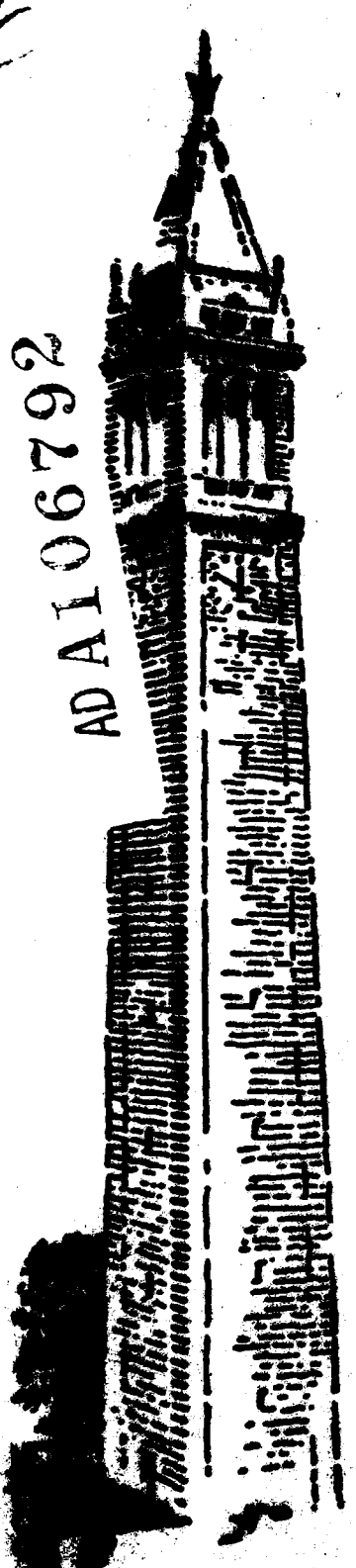

LEVEL II

10

ALGORITHMS FOR COMPUTING ALMOST-PERIODIC STEADY-STATE RESPONSE OF NONLINEAR SYSTEMS TO MULTIPLE INPUT FREQUENCIES

by

L. O. Chua and A. Ushida

Memorandum No. UCB/ERL M80/55

16 December 1980

ELECTRONICS RESEARCH LABORATORY
College of Engineering
University of California, Berkeley, CA 94720

ALGORITHMS FOR COMPUTING ALMOST-PERIODIC STEADY-STATE RESPONSE OF NONLINEAR SYSTEMS TO MULTIPLE INPUT FREQUENCIES

by

L. O. Chua [redacted] A. Ushida

Memorandum No. UCB/ERL-M80/55

16 Dec[redacted]80

ELECTRONICS RESEARCH LABORATORY

College of Engineering
University of California, Berkeley
94720

ALGORITHMS FOR COMPUTING ALMOST-PERIODIC STEADY-STATE RESPONSE OF NONLINEAR SYSTEMS TO MULTIPLE INPUT FREQUENCIES[†]

L. O. Chua and A. Ushida[§]

ABSTRACT

Two efficient algorithms are presented for obtaining steady-state solutions of nonlinear circuits and systems driven by two or more distinct frequency input signals. These algorithms are particularly useful in cases where the steady-state response is either not periodic, or is periodic but its period is too large for existing methods.

The first algorithm is applicable to any circuit or system driven by any number $P \geq 2$ of input frequencies. The second algorithm is restricted only to 2 input frequencies and is therefore significantly more efficient than the first algorithm. Both algorithms are formulated for systems described by an implicit system of nonlinear algebraic-differential equations, thereby obviating the need to write state equations.

Numerous examples have been solved successfully using these two algorithms. A selection of some of these examples is given for illustrative purposes.

[†]Research supported in part by the Office of Naval Research under Contract N00014-76-0572 and the National Science Foundation under Grant ENG75-22282.

[§]L. O. Chua is with the Department of Electrical Engineering and Computer Sciences and the Electronics Research Laboratory at the University of California, Berkeley, California 94720.

A. Ushida is with the Department of Electrical Engineering, Faculty of Engineering, Tokushima University, Tokushima, Japan.

I. Introduction

A fundamental problem in the design of communication circuits, such as modulators and mixers, is to calculate the steady-state response when the circuit is driven by inputs having "P" distinct frequency components $\{\omega_1,\omega_2,\ldots,\omega_p\}$, where $P \geq 2$ [1-2]. For complete generality, we assume the circuit or system is described by an implicit system of differential-algebraic equations [3] of the form

$$f_j(\dot{\underset{\sim}{x}},\underset{\sim}{x},\underset{\sim}{y};\omega_1 t,\omega_2 t,\ldots\omega_p t) = 0 \quad , \; j = 1,2,\ldots,m+n \tag{1.1}$$

where $\underset{\sim}{x}$ is an n-vector denoting the state variables, $\underset{\sim}{y}$ is an m-vector denoting the remaining non-state variables and $f_j(\cdot)$ contains p periodic input signals of frequencies $\omega_1,\omega_2,\ldots,\omega_p$, respectively. In Appendix A, $f_j(\cdot)$ is given by an explicit formula which holds for most circuits of practical interest.

Standing Assumption. Given any initial state $\underset{\sim}{x}_0$, (1.1) has a unique asymptotically almost-periodic solution [4]; namely,

$$\underset{\sim}{x}(t) = \underset{\sim}{x}_{tr}(t) + \underset{\sim}{x}_{ss}(t) \tag{1.2}$$

where

$$\underset{\sim}{x}_{tr}(t) \to \underset{\sim}{0} \text{ as } t \to \infty \tag{1.3}$$

is called the transient component and

$$\underset{\sim}{x}_{ss}(t) = \underset{\sim}{a}_0 + \sum_{k=1}^{M} \left\{ \underset{\sim}{a}_{2k-1} \cos \nu_k t + \underset{\sim}{a}_{2k} \sin \nu_k t \right\} \tag{1.4}$$

is called the steady state response , where the summation is taken over all possible frequencies [5]

$$\boxed{\nu_k \triangleq m_{1k}\omega_1 + m_{2k}\omega_2 + \ldots + m_{pk}\omega_p} \tag{1.5}$$

generated by the frequency base $\omega_1,\omega_2,\ldots,\omega_p$.

Note that (1.4) is not an ordinary Fourier series because its frequency spectrum $\{\nu_1,\nu_2,\ldots,\nu_M\}$ is not harmonically related. In fact, $\underset{\sim}{x}_{ss}(t)$ is not even periodic if the frequency base $\{\omega_1,\omega_2,\ldots,\omega_p\}$ is incommensurable [5]. In the mathematical literature, (1.4) is called an almost periodic function.

Our objective in this paper is to present 2 efficient algorithms for calculating the steady-state response $\underset{\sim}{x}_{ss}(t)$.

Current methods for calculating $\underset{\sim}{x}_{ss}(t)$ can be classified into 4 categories:

1. Brute force method. This approach solves (1.1) by numerical integration (starting from an arbitrarily chosen initial state $\underset{\sim}{x}_0$) until the steady state is reached [3].

Although this method is quite general, it is prohibitively expensive for lightly-damped circuits where it takes a very long time for the transient component to die out.

Moreover, if the frequency base is incommensurable, $\underset{\sim}{x}_{ss}(t)$ is not periodic and it is difficult to determine when the steady state has been reached.

2. Perturbation method. This approach solves (1.1) by iteration with the initial solution often chosen to be the solution of a linearized equation. It includes the Volterra series method [5-7] and the Picard iteration method [8].

Unfortunately, this method works only for almost linear circuits where the nonlinearity is often extremely weak (e.g., low distortion amplifiers). For circuits which rely on nonlinearity in an essential way (e.g., modulators and mixers) this method becomes highly inaccurate let alone the fact that the iteration often does not converge.

3. Harmonic balance method. This approach solves (1.1) by approximating the solution in a finite trigonometric series and then balancing all terms having identical frequency components, often via Galerkin's procedure [9-10].

Although very interesting theoretically, this method is often extremely time-consuming because the various frequency components are estimated by multi-dimensional Fourier analysis.

4. Shooting method. This approach solves (1.1) by finding first an initial state $\underset{\sim}{x}_0$ (often via Newton-Raphon method) such that the solution starting from $\underset{\sim}{x}_0$ is periodic, i.e., no transient component [11-12].

There are 2 serious problems associated with this method.

(a) It can not be used when the solution is not periodic.

(b) Even if the solution is periodic, the period T is often many orders of magnitude larger than the period of the individual frequency components ν_k, thereby making the numerical integration over this long period T prohibitively expensive. For example, consider

$$x_{ss}(t) = A_1 \cos \omega_1 t + A_2 \cos \omega_2 t \tag{1.6}$$

The following table lists several combinations of ω_1 and ω_2 (of periods T_1 and T_2 respectively) which makes $x_{ss}(t)$ a periodic function. Also listed is the period T of $x_{ss}(t)$ and the ratio $\rho_1 \triangleq T/T_1$ and $\rho_2 = T/T_2$.

Table 1. Example of ω_1 and ω_2 which make $x_{ss}(t)$ periodic of frequency ω.

ω_1(Hz)	ω_2(Hz)	$T_1 = \frac{2\pi}{\omega_1}$(sec)	$T_2 = \frac{2\pi}{\omega_2}$(sec)	$T = \frac{2\pi}{\omega}$(sec)	$\rho_1 \triangleq \frac{T}{T_1}$	$\rho_2 \triangleq \frac{T}{T_2}$
1	0.23	6.2832	27.318	$6.2832(10^2)$	10^2	$0.23(10^2)$
1	0.233	6.2832	26.967	$6.2832(10^3)$	10^3	$0.233(10^3)$
1	0.2333	6.2832	26.932	$6.2832(10^4)$	10^4	$0.2333(10^4)$
1	$\underbrace{0.2333\ldots3}_{n \text{ digits}}$	6.2832	26.927	$6.2832(10^n)$	10^n	$\underbrace{0.233\ldots3(10^n)}_{n \text{ digits}}$
10^3	$0.233(10^3)$	$6.2832(10^{-3})$	$0.26967(10^{-3})$	6.2832	10^3	$0.233(10^3)$
10^4	$0.2333(10^4)$	$6.2832(10^{-4})$	$0.26932(10^{-4})$	6.2832	10^4	$0.2333(10^4)$
10^5	$0.23333(10^5)$	$6.2832(10^{-5})$	$0.26932(10^{-5})$	6.2832	10^5	$0.23333(10^5)$
10^n	$\underbrace{0.23333\ldots3(10^n)}_{n \text{ digits}}$	$6.2832(10^{-n})$	$0.26927(10^{-n})$	6.2832	10^n	$\underbrace{0.233\ldots3(10^n)}_{n \text{ digits}}$

Note that when $\omega_1 = 1$, $T \to \infty$ as $n \to \infty$, and when $\omega_1 = 10^n$, $T_1 \to 0$ but $T = 6.2832$ as $n \to \infty$. Hence, from a numerical integration point of view, it will take an infinite amount of integration steps in order to obtain the periodic solution $x_{ss}(t)$ when $n \to \infty$. Since $\rho_1 \to \infty$ and $\rho_2 \to \infty$ as $n \to \infty$ *in both cases*, the larger the values of ρ_1 and ρ_2, the more computer time will be required. Hence, ρ_1 and ρ_2 give a measure of numerical efficiency of the shooting method. This observation motivates *the following:*

Theorem 1

The steady state response $\underset{\sim}{x}_{ss}(t)$ in (1.4) is periodic of frequency ω if each frequency ν_k can be expressed as a rational number

$$\nu_k = \frac{m_k}{n_k}, \quad k = 1,2,\ldots,M \tag{1.6}$$

Moreover, if m_k and n_k are relatively prime integers for all $k = 1,2,\ldots,M$, then the period $T \triangleq 2\pi/\omega$ of $\underset{\sim}{x}_{ss}(t)$ is given explicitly by

$$\boxed{T = 2\pi\left(\frac{n}{m}\right)} \tag{1.7}$$

where[†]

$$n \triangleq \text{L.C.M.}\ \{n_1,n_2,\ldots,n_M\} \tag{1.8}$$

$$m \triangleq \text{G.C.D.}\ \{m_1,m_2,\ldots,m_M\} \tag{1.9}$$

[†]L.C.M. and G.C.D. denote Least Common Multiple and Greatest Common Divisor, respectively.

and

$$\rho_k \triangleq \frac{T}{T_k} = \left(\frac{n}{m}\right)\nu_k \tag{1.10}$$

where $T_k = 2\pi/\nu_k$.

Conversely, if there are at least 2 frequencies ν_j and ν_k where ν_j is rational but ν_k is irrational, then $\underset{\sim}{x}_{ss}(t)$ is not periodic.

Proof. Rewriting (1.4) as

$$\underset{\sim}{x}_{ss}(t) = \underset{\sim}{x}_{ss}(\nu_1 t, \nu_2 t, \ldots, \nu_M t) \tag{1.11}$$

to emphasize the M periodic components of frequency $\nu_1, \nu_2, \ldots, \nu_M$, we obtain

$$\begin{aligned}
\underset{\sim}{x}_{ss}(t+T) &= \underset{\sim}{x}_{ss}\{\nu_1(t+T), \nu_2(t+T), \ldots, \nu_M(t+T)\} \\
&= \underset{\sim}{x}_{ss}\{\nu_1(t+2\pi(\tfrac{n}{m})), \nu_2(t+2\pi(\tfrac{n}{m})), \ldots, \nu_M(t+2\pi(\tfrac{n}{m}))\} \\
&= \underset{\sim}{x}_{ss}\{\nu_1(t+\nu_1(\tfrac{n}{m})(\tfrac{2\pi}{\nu_1})), \nu_2(t+\nu_2(\tfrac{n}{m})(\tfrac{2\pi}{\nu_2})), \ldots, \nu_M(t+\nu_M(\tfrac{n}{m})(\tfrac{2\pi}{\nu_M}))\} \\
&= \underset{\sim}{x}_{ss}\{\nu_1(t+\tfrac{m_1}{n_1}(\tfrac{n}{m})T_1), \nu_2(t+\tfrac{m_2}{n_2}(\tfrac{n}{m})T_2), \ldots, \nu_M(t+\tfrac{m_M}{n_M}(\tfrac{n}{m})T_M)\} \\
&= \underset{\sim}{x}_{ss}\{\nu_1(t+N_1T_1), \nu_2(t+N_2T_2), \ldots, \nu_M(t+N_MT_M)\}
\end{aligned} \tag{1.12}$$

where

$$N_k \triangleq \frac{m_k}{n_k}(\frac{n}{m}) = (\frac{m_k}{m})(\frac{n}{n_k}),\ k = 1,2,\ldots,M \tag{1.13}$$

is an integer in view of (1.8) and (1.9). It follows from (1.13) and (1.4) that

$$\underset{\sim}{x}_{ss}(t+T) = \underset{\sim}{x}_{ss}(\nu_1 t, \nu_2 t, \ldots, \nu_M t) = \underset{\sim}{x}_{ss}(t) \tag{1.14}$$

Hence $\underset{\sim}{x}_{ss}(t)$ is periodic of period T. Moreover, since m_k and n_k are relatively prime, T is the smallest period and hence, $T = 2\pi/\omega$.

Finally, if ν_j is rational but ν_k is irrational, we can represent ν_k by (1.6) with $n_k \to \infty$. Consequently, $n = \text{L.C.M.}\{n_1, \ldots n_j, \ldots, n_k, \ldots n_M\} = \infty$ and $\underset{\sim}{x}_{ss}(t)$ has an infinite period; i.e., it is not periodic. ■

It follows from Theorem 1 that if $\underset{\sim}{x}_{ss}(t)$ is periodic, its frequency is given by

$$\boxed{\omega = \frac{m}{n} = \frac{\text{G.C.D.}\{m_1, m_2, \ldots, m_M\}}{\text{L.C.M.}\{n_1, n_2, \ldots, n_M\}}} \tag{1.15}$$

and its period T is bounded by:

$$\max\{T_1, T_2, .., T_p\} \leq T \leq 2\pi(n_1 n_2 \ldots n_M) \tag{1.16}$$

It also follows from (1.8)-(1.10) that since m is typically a small integer (m=1 if all m_k are relatively prime), the period T can be many orders of magnitude larger than that of T_k. Typically, T increases by an order of magnitude if we increase the number of significant figures in representing the component frequencies ν_k, k = 1,2,...,p by one.

Observe that in solving (1.1) by numerical integration, the step size h is determined by the period of the highest frequency component [3], namely,

$$h \leq \frac{1}{8} \min\{T_1, T_2, \ldots, T_k\} \tag{1.17}$$

It follows from (1.16) and (1.17) that both the brute force method and the shooting method are usually impractical when there are multiple input frequencies.

To overcome the problems associated with existing methods, we will present two new efficient algorithms in this paper. The basic idea in both algorithms is to find an initial state $\underset{\sim}{x}(0) \triangleq \underset{\sim}{x}_0^*$ so that the transient component

$$\underset{\sim}{x}_{tr}(t) = \underset{\sim}{0} \text{ for all } t \geq 0 \tag{1.18}$$

regardless of whether the steady state response $\underset{\sim}{x}_{ss}(t)$ is periodic or not. In both algorithms, $\underset{\sim}{x}_0^*$ is found by a Newton-Raphson mehtod. However, unlike the shooting method [11], (1.3) is solved numerically only over a small fraction of the period T (in the periodic case) per iteration. This is why our algorithms are computationally quite efficient.

The algorithm to be presented in Section II is completely general and is applicable regardless of the number "p" of input frequencies, provided $p < \infty$.

The algorithm to be presented in Section III is restricted only to the 2-input frequency case (p=2). We will see that this restriction leads to a significantly more efficient algorithm than that of Section II.

II. Almost-Periodic Solution Algorithm 1: Multiple-Input Frequencies

Since our algorithm does not depend on whether $\underset{\sim}{x}_{ss}(t)$ is periodic or not, let us assume that the exact steady-state response

$$\boxed{\underset{\sim}{x}_{ss}(t) = \underset{\sim}{a}_0 + \sum_{k=1}^{M} \{\underset{\sim}{a}_{2k-1} \cos \nu_k t + \underset{\sim}{a}_{2k} \sin \nu_k t\}} \tag{2.1}$$

is not periodic for the sake of generality. Consequently, we will call the coefficients $\underset{\sim}{a}_k$ as generalized Fourier coefficients.

Even though the number M of frequency components in (2.1) could be quite large (M may equal ∞!) in most practical cases,

$$A_k \triangleq \sqrt{\|\underset{\sim}{a}_{2k-1}\|^2 + \|\underset{\sim}{a}_{2k}\|^2} \approx 0 \quad \text{for all } k > N \tag{2.2}$$

where $\|\cdot\|$ denotes Euclidean norm.

Hence, we will seek to find an approximate solution

$$\boxed{\underset{\sim}{x}_N(t) = \underset{\sim}{a}_0 + \sum_{k=1}^{N} \{\underset{\sim}{a}_{2k-1} \cos \nu_k t + \underset{\sim}{a}_{2k} \sin \nu_k t\}} \tag{2.3}$$

whose $N < M$.

A. Calculating $\underset{\sim}{a}_k$ when transient component is zero

In section II-B, we will present an algorithm for finding an initial state $\underset{\sim}{x}_0^*$ such that the transient solution component $\underset{\sim}{x}_{tr}(t)$ in (1.3) is zero for $t \geq 0$. In this subsection, let us assume $\underset{\sim}{x}_0^*$ has been found so that the solution of (1.1) starting from $\underset{\sim}{x}_0^*$ is $\underset{\sim}{x}(t) = \underset{\sim}{x}_{ss}(t)$ for $t \geq 0$.

To minimize computation time, we will often choose a relatively small N so that (2.2) is not necessarily satisfied. In this case, the following theorem is important:

Theorem 2. Properties of Generalized Fourier Coefficients

Let $N < M$ be any positive integer.

(a) For any (not necessarily optimum) N-frequency component approximation

$$\bar{\underset{\sim}{x}}_N(t) \triangleq \underset{\sim}{b}_0 + \sum_{k=1}^{N} \{\underset{\sim}{b}_{2k-1} \cos \nu_k t + \underset{\sim}{b}_{2k} \sin \nu_k t\} \tag{2.4}$$

to $\underset{\sim}{x}_{ss}(t)$ in (2.1), the mean-square error

$$M[\underset{\sim}{x}_{ss}(t) - \bar{\underset{\sim}{x}}_N(t)]^2 \triangleq \lim_{T\to\infty} \frac{1}{T} \int_0^T \|\underset{\sim}{x}_{ss}(t) - \underset{\sim}{x}_N(t)\|^2 dt$$

is given explicitly by:†

†We define the mean of x(t) by

$$M\{x(t)\} \triangleq \lim_{T\to\infty} \frac{1}{T} \int_0^T x(t)dt$$

$$M[\underset{\sim}{x}_{ss}(t)-\overline{\underset{\sim}{x}}_N(t)]^2 = M[\underset{\sim}{x}_{ss}(t)]^2 - \|\underset{\sim}{a}_0\|^2 - \frac{1}{2}\sum_{k=1}^{N}\|\underset{\sim}{a}_k\|^2 + \|\underset{\sim}{a}_0-\underset{\sim}{b}_0\|^2 + \frac{1}{2}\sum_{k=1}^{N}\|\underset{\sim}{a}_k-\underset{\sim}{b}_k\|^2 \quad (2.5)$$

(b) Among all possible coefficients $\{\underset{\sim}{b}_0,\underset{\sim}{b}_1,\ldots,\underset{\sim}{b}_{2N}\}$ in (2.4), the coefficients which result in a minimum mean-square error are precisely the first 2N+1 generalized Fourier coefficients; namely

$$\underset{\sim}{b}_k = \underset{\sim}{a}_k,\ k = 0,1,2,\ldots,2N \quad (2.6)$$

(c) The minimum mean-square-error is given by:

$$M[\underset{\sim}{x}_{ss}(t)-\underset{\sim}{x}_N(t)]^2 = \frac{1}{2}\sum_{k=N+1}^{M}\|\underset{\sim}{a}_k\|^2 \quad (2.7)$$

Proof. It suffices to prove the scalar case.

$$\text{(a)}\quad M[x_{ss}(t)-\overline{x}_N(t)]^2 = M\{x_{ss}(t) - b_0 - \sum_{k=1}^{N}[b_{2k-1}\cos\nu_k t+b_{2k}\sin\nu_k t]\}^2$$

$$= M[x_{ss}(t)]^2 - 2b_0M[x_{ss}(t)] - 2M\{x_{ss}(t)\sum_{k=1}^{N}[b_{2k-1}\cos\nu_k t+b_{2k}\sin\nu_k t]\}$$

$$+ b_0^2 + M\{\sum_{k=1}^{N}[b_{2k-1}\cos\nu_k t+b_{2k}\sin\nu_k t]\}^2 \quad (2.8)$$

where we have made use of the fact that

$$M\{\sin\nu t\} = 0 \quad \text{for all } \nu \quad (2.9)$$

$$M\{\cos\nu t\} = 0 \quad \text{for all } \nu \neq 0 \quad (2.10)$$

The last term in (2.8) can be further reduced:

$$M\{\sum_{k=1}^{N}[b_{2k-1}\cos\nu_k t+b_{2k}\sin\nu_k t]\}^2 = \frac{1}{2}\sum_{k=1}^{N}(b_{2k-1}^2+b_{2k}^2) = \frac{1}{2}\sum_{k=1}^{2N}b_k^2 \quad (2.11)$$

Substituting (2.1) for $x_{ss}(t)$ in the second and third terms in (2.8), we obtain

$$2b_0M[x_{ss}(t)] + 2M\{x_{ss}(t)\sum_{k=1}^{N}[b_{2k-1}\cos\nu_k t+b_{2k}\sin\nu_k t]\}$$

$$= 2a_0b_0 + \sum_{k=1}^{N}(b_{2k-1}a_{2k-1}+b_{2k}a_{2k}) = 2a_0b_0 + \sum_{k=1}^{2N}a_kb_k \quad (2.12)$$

Substituting (2.11) and (2.12) into (2.8), we obtain:

$$M[x_{ss}(t)-\overline{x}_N(t)]^2 = M[x_{ss}(t)]^2 - 2a_0b_0 - \sum_{k=1}^{2N}a_kb_k + b_0^2 + \frac{1}{2}\sum_{k=1}^{2N}b_k^2$$

$$= M[x_{ss}(t)]^2 - a_0^2 - \frac{1}{2}\sum_{k=1}^{2N}a_k^2 + (a_0-b_0)^2 + \frac{1}{2}\sum_{k=1}^{2N}(a_k-b_k)^2 \quad (2.13)$$

which is just the scalar version of (2.5).

(b) Since b_k occurs only in the last 2 terms of (2.13), the minimum of (2.13) occurs when (2.6) holds.

(c) $$M[x_{ss}(t)]^2 = a_0^2 + \frac{1}{2}\sum_{k=1}^{M} a_k^2 \tag{2.14}$$

Substituting (2.6) and (2.14) into (2.13), we obtain:

$$M[x_{ss}(t)-x_N(t)]^2 = \frac{1}{2}\sum_{k=N+1}^{M} a_k^2 \tag{2.15}$$

which is just the scalar version of (2.7). ■

Theorem 2 shows that regardless of the integer N, the generalized Fourier coefficients $\{\underset{\sim}{a}_0,\underset{\sim}{a}_1,\ldots,\underset{\sim}{a}_{2N}\}$ in (2.3) can be obtained by minimizing the means-square-error between $\underset{\sim}{x}_{ss}(t)$ and $\underset{\sim}{x}_N(t)$. Hence, increasing the number of frequency components from N to N+1 does not affect the previously calculated coefficients.

Since by assumption, $\underset{\sim}{x}_{tr}(t) = \underset{\sim}{0}$ *for* $t \geq 0$, we can calculate $\underset{\sim}{x}_{ss}(t)$ by solving (1.2) numerically. Assuming a uniform step size Δt, let us calculate (Z+1) time steps to obtain $\underset{\sim}{x}_{ss}(\Delta t)$, $\underset{\sim}{x}_{ss}(2\Delta t),\ldots,\underset{\sim}{x}_{ss}(k\Delta t),\ldots,\underset{\sim}{x}_{ss}((Z+1)\Delta t)$, where Z is some integer to be chosen later.

Since Theorem 2 implies that the jth components a_{kj}, k = 0,1,...,2N, of each generalized *Fourier coefficient* $\underset{\sim}{a}_k$ *can be determined independently* of the coefficients of the remaining components of the vector $\underset{\sim}{x}_N(t)$, it suffices for us to derive a formula for calculating these coefficients in the scalar case. To simplify our notation, define the vectors

$$\underset{\sim}{x}_{ss}(Z) \triangleq \begin{bmatrix} x_{ss}(0) \\ x_{ss}(\Delta t) \\ x_{ss}(2\Delta t) \\ \vdots \\ x_{ss}(Z\Delta t) \end{bmatrix}, \underset{\sim}{x}_N(Z) \triangleq \begin{bmatrix} x_N(0) \\ x_N(\Delta t) \\ x_N(2\Delta t) \\ \vdots \\ x_N(Z\Delta t) \end{bmatrix}, \underset{\sim}{a} \triangleq \begin{bmatrix} a_0 \\ a_1 \\ a_2 \\ \vdots \\ a_{2N} \end{bmatrix}, \text{ and } \hat{\underset{\sim}{a}}(Z) \triangleq \begin{bmatrix} \hat{a}_0(Z) \\ \hat{a}_1(Z) \\ \hat{a}_2(Z) \\ \vdots \\ \hat{a}_{2N}(Z) \end{bmatrix} \tag{2.16}$$

and the Z × (2N+1) matrix

$$\underset{\sim}{\Gamma} \triangleq \begin{bmatrix} 1 & 1 & 0 & \ldots & 1 & 0 \\ 1 & \cos \nu_1\Delta t & \sin \nu_1\Delta t & \ldots & \cos \nu_N\Delta t & \sin \nu_N\Delta t \\ 1 & \cos 2\nu_1\Delta t & \sin 2\nu_1\Delta t & \ldots & \cos 2\nu_N\Delta t & \sin 2\nu_N\Delta t \\ \vdots & & \vdots & & \vdots & \vdots \\ 1 & \cos Z\nu_1\Delta t & \sin Z\nu_1\Delta t & \ldots & \cos Z\nu_N\Delta t & \sin Z\nu_N\Delta t \end{bmatrix} \tag{2.17}$$

Theorem 3

The (2N+1) generalized Fourier coefficients $\{a_0, a_1, \ldots, a_k, \ldots, a_{2N}\}$ of $x_N(t)$ (scalar version of (2.3)) are given by

$$\underset{\sim}{a} = \hat{\underset{\sim}{a}}(Z) + \underset{\sim}{\varepsilon}(Z) \tag{2.18}$$

where

$$\boxed{\hat{\underset{\sim}{a}}(Z) \triangleq (\underset{\sim}{\Gamma}^T \underset{\sim}{\Gamma})^{-1} \underset{\sim}{\Gamma}^T \underset{\sim}{x}_{ss}(Z)} \tag{2.19}$$

and $\underset{\sim}{\varepsilon}(Z)$ is an error vector satisfying

$$\underset{\sim}{\varepsilon}(Z) \to \underset{\sim}{0} \quad \text{as } Z \to \infty \tag{2.20}$$

The (2N+1) × (2N+1) matrix $(\underset{\sim}{\Gamma}^T \underset{\sim}{\Gamma})$ in (2.19) is non-singular for all positive frequencies $\nu_1, \nu_2, \ldots, \nu_N$ and for any step size Δt if, and only if

$$\Delta t \neq \frac{2n\pi}{|\nu_i \pm \nu_k|} \tag{2.21}$$

for all i, k = 1,2,...,N, and for any integer n.

Proof.

$$\begin{aligned} M[x_{ss}(t)-x_N(t)]^2 &= \lim_{T\to\infty} \frac{1}{T} \int_0^T [x_{ss}(t)-x_N(t)]^2 \, dt \\ &= \lim_{Z\to\infty} \frac{1}{(Z+1)\Delta t} \left\{ \sum_{k=0}^{Z} [x_{ss}(k\Delta t)-x_N(k\Delta t)]^2 \, \Delta t \right\} \\ &= \frac{1}{(Z+1)} \left\{ \sum_{k=0}^{Z} [x_{ss}(k\Delta t)-x_N(k\Delta t)]^2 \right\} + \varepsilon(Z) \end{aligned} \tag{2.22}$$

where

$\varepsilon(Z) \geq 0$ denotes the error resulting from taking only a finite number Z of time steps.

Now substituting $t = k\Delta t$ in (2.3) and using the notations in (2.16) and (2.17), we can write

$$\begin{aligned} \sum_{k=0}^{Z} [x_{ss}(k\Delta t)-x_N(k\Delta t)]^2 &= [\underset{\sim}{x}_{ss}(Z)-\underset{\sim}{x}_N(Z)]^T [\underset{\sim}{x}_{ss}(Z)-\underset{\sim}{x}_N(Z)] \\ &= [\underset{\sim}{x}_{ss}(Z)-\underset{\sim}{\Gamma}\hat{\underset{\sim}{a}}(Z)]^T [\underset{\sim}{x}_{ss}(Z)-\underset{\sim}{\Gamma}\hat{\underset{\sim}{a}}(Z)] \\ &= \underset{\sim}{x}_{ss}^T(Z)\underset{\sim}{x}_{ss}(Z) - \hat{\underset{\sim}{a}}^T(Z)\underset{\sim}{\Gamma}^T\underset{\sim}{x}_{ss}(Z) - \underset{\sim}{x}_{ss}^T(Z)\underset{\sim}{\Gamma}\hat{\underset{\sim}{a}}(Z) \\ &\quad + \hat{\underset{\sim}{a}}^T(Z)\underset{\sim}{\Gamma}^T\underset{\sim}{\Gamma}\hat{\underset{\sim}{a}}(Z) \end{aligned} \tag{2.23}$$

After adding and subtracting $\underset{\sim}{\sigma}^T\underset{\sim}{G}^{-1}\underset{\sim}{G}\underset{\sim}{G}^{-1}\underset{\sim}{\sigma} = \underset{\sim}{S}^T\underset{\sim}{G}^{-1}\underset{\sim}{\sigma}$ to (2.23), where

$$\underset{\sim}{G} \triangleq \underset{\sim}{\Gamma}^T\underset{\sim}{\Gamma} \quad \text{and} \quad \underset{\sim}{\sigma} \triangleq \underset{\sim}{\Gamma}^T\underset{\sim}{x}_{ss}(Z) \tag{2.24}$$

we obtain

$$\sum_{k=0}^{Z}[x_{ss}(k\Delta t)-x_N(k\Delta t)]^2 = \underset{\sim}{x}_{ss}^T(Z)\underset{\sim}{x}_{ss}(Z) - \hat{\underset{\sim}{a}}^T(Z)\underset{\sim}{G}\underset{\sim}{G}^{-1}\underset{\sim}{\sigma} - \underset{\sim}{\sigma}^T\underset{\sim}{G}\underset{\sim}{G}^{-1}\hat{\underset{\sim}{a}}(Z) + \hat{\underset{\sim}{a}}^T(Z)\underset{\sim}{G}\hat{\underset{\sim}{a}}(Z)$$

$$+ \underset{\sim}{\sigma}^T\underset{\sim}{G}^{-1}\underset{\sim}{G}\underset{\sim}{G}^{-1}\underset{\sim}{\sigma} - \underset{\sim}{\sigma}^T\underset{\sim}{G}^{-1}\underset{\sim}{\sigma}$$

$$= (\hat{\underset{\sim}{a}}(Z)-\underset{\sim}{G}^{-1}\underset{\sim}{\sigma})^T\underset{\sim}{G}\,(\hat{\underset{\sim}{a}}(Z)-\underset{\sim}{G}^{-1}\underset{\sim}{\sigma}) + \underset{\sim}{x}_{ss}^T(Z)\underset{\sim}{x}_{ss}(Z) - \underset{\sim}{\sigma}^T\underset{\sim}{G}^{-1}\underset{\sim}{\sigma} \tag{2.25}$$

Since only the first term of (2.25) depends on $\hat{\underset{\sim}{a}}(Z)$, and since $\underset{\sim}{G}$ as defined in (2.24) is clearly positive semi-definite, it follows from (2.22) and (2.25) that the mean-square error $M[x_{ss}(t)-x_N(t)]^2$ attains its minimum when

$$\hat{\underset{\sim}{a}}(Z) = \underset{\sim}{G}^{-1}\underset{\sim}{\sigma} = (\underset{\sim}{\Gamma}^T\underset{\sim}{\Gamma})^{-1}\underset{\sim}{\Gamma}^T\underset{\sim}{x}_{ss}(Z) \tag{2.26}$$

It follows from Theorem 2 that as $Z \to \infty$, $\hat{\underset{\sim}{a}}(Z) \to \underset{\sim}{a}$ and hence $\underset{\sim}{\epsilon}(Z) \to \underset{\sim}{0}$ in (2.18).

The proof showing $(\underset{\sim}{\Gamma}^T\underset{\sim}{\Gamma})$ is nonsingular if and only if (2.21) holds involves some cumbersome determinant expansions. The details are given in Appendix B. ∎

Theorem 3 gives us an explicit formula for calculating (approximately) the (2N+1) generalized Fourier coefficients $\{a_0,a_1,\ldots,a_{2N}\}$ for any N; namely,

$$\boxed{\underset{\sim}{a} \simeq (\underset{\sim}{\Gamma}^T\underset{\sim}{\Gamma})^{-1}\underset{\sim}{\Gamma}^T\,\underset{\sim}{x}_{ss}(Z)} \tag{2.27}$$

This approximate formula becomes exact as the number Z of integration time steps tends to ∞.

Since (2.21) applies only at a countable set of isolated points, it is easy to choose a suitable Δt satisfying (2.21). Once Δt is chosen, $\underset{\sim}{\Gamma}$ can be calculated from (2.17). The vector $\underset{\sim}{x}_{ss}(Z)$ in (2.17) represents (2N+1) "samples" taken from the exact steady-state solution $\underset{\sim}{x}_{ss}(t)$ from (2.1) at a regular time interval equal to Δt.

In practice, $\underset{\sim}{x}_{ss}(Z)$ is of course calculated numerically by solving (1.1) starting from any initial state $\underset{\sim}{x}_0^*$ which results in a zero transient component.†

Finally, note that (2.27) gives the (2N+1) generalized Fourier coefficients of only one component of the state vector $\underset{\sim}{x}_{ss}(t)$. Hence, (2.27) must be applied

†This implicit system of differential-algebraic equations can be solved using the Backward Differentiation Formula (BDF) as described in [3].

n times for the "n" state variables in $\underset{\sim}{x}$. Since $\underset{\sim}{\Gamma}$ remains unchanged, each calculation involves only changing $\underset{\sim}{x}_{ss}(Z)$ in (2.27) corresponding to <u>each component</u> of $\underset{\sim}{x}_{ss}(t)$.

B. <u>Finding the initial state $\underset{\sim}{x}_0^*$</u>

If we let $x_{N_i}(T_b)$ denote the <u>i</u>th component of $\underset{\sim}{x}_N(t)$ from (2.3) at any time $t = T_b$, then

$$x_{N_i}(T_b) = a_{0_i} + \sum_{k=1}^{N} \{a_{2k-1_i} \cos \nu_k T_b + a_{2k_i} \sin \nu_k T_b\} \tag{2.28}$$

when a_{k_i} denotes the <u>i</u>th component of $\underset{\sim}{a}_k$. Substituting (2.27) for $\underset{\sim}{a}_i$ in (2.28), we obtain

$$x_{N_i}(T_b) \approx \underset{\sim}{\gamma}^T(T_b)\underset{\sim}{a}_i = \underset{\sim}{\gamma}^T(T_b)[(\underset{\sim}{\Gamma}^T\underset{\sim}{\Gamma})^{-1}\underset{\sim}{\Gamma}^T\underset{\sim}{x}_{ss_i}(Z)] = \underset{\sim}{x}_{ss_i}^T(Z)\,[\underset{\sim}{\Gamma}(\underset{\sim}{\Gamma}^T\underset{\sim}{\Gamma})^{-1}\underset{\sim}{\gamma}(T_b)],$$

$$i = 1,2,\ldots,n \tag{2.29}$$

where $\underset{\sim}{x}_{ss_i}^T(Z)$ denotes the $\underset{\sim}{x}_{ss}(Z)$ (as defined in (2.16)) associated with the <u>i</u>th component of $\underset{\sim}{x}_{ss}(t)$, and

$$\boxed{\underset{\sim}{\gamma}(T_b) \triangleq [1 \;\cos \nu_1 T_b \quad \sin \nu_1 T_b, \ldots, \cos \nu_N T_b \quad \sin \nu_N T_b]^T} \tag{2.30}$$

Since $\underset{\sim}{\Gamma}(\underset{\sim}{\Gamma}^T\underset{\sim}{\Gamma})^{-1}\underset{\sim}{\gamma}(T_b)$ in (2.29) remains unchanged for all $i = 1,2,\ldots,n$, we can combine all n components of $\underset{\sim}{x}_N(t)$ from (2.29) into a single matrix equation:

$$\underbrace{\begin{bmatrix} x_{N_1}(T_b) \\ x_{N_2}(T_b) \\ \vdots \\ x_{N_n}(T_b) \end{bmatrix}}_{\underset{\sim}{x}_N(T_b;\underset{\sim}{x}_0^*)} \approx \underbrace{\begin{bmatrix} x_{ss_1}(0) & x_{ss_1}(\Delta t) & x_{ss_1}(2\Delta t) & \ldots & x_{ss_1}(Z\Delta t) \\ x_{ss_2}(0) & x_{ss_2}(\Delta t) & x_{ss_2}(2\Delta t) & \ldots & x_{ss_2}(Z\Delta t) \\ \vdots & \vdots & \vdots & \vdots\vdots & \vdots \\ x_{ss_n}(0) & x_{ss_n}(\Delta t) & x_{ss_n}(2\Delta t) & \ldots & x_{ss_n}(Z\Delta t) \end{bmatrix}}_{\underset{\sim}{X}(\Delta t,Z;\,\underset{\sim}{x}_0^*)} \underbrace{\begin{bmatrix} \alpha_0(T_b;\Delta t,Z,N) \\ \alpha_1(T_b;\Delta t,Z,N) \\ \alpha_2(T_b;\Delta t,Z,N) \\ \vdots \\ \alpha_Z(T_b;\Delta t,Z,N) \end{bmatrix}}_{\underset{\sim}{\alpha}(T_b;\Delta t,Z,N)} \tag{2.31}$$

where the (Z+1)-vector

$$\boxed{\underset{\sim}{\alpha}(T_b;\Delta t,Z,N) \triangleq \underset{\sim}{\Gamma}(\underset{\sim}{\Gamma}^T\underset{\sim}{\Gamma})^{-1}\underset{\sim}{\gamma}(T_b)} \tag{2.32}$$

depends <u>only</u> on T_b, Δt, Z, and N (since $\underset{\sim}{\Gamma}$ in (2.17) depends on Δt, Z, and N) but <u>not</u> on $\underset{\sim}{x}_0^*$.

We can recast (2.31) into an exact equation by introducing a slack variable $\underset{\sim}{\varepsilon}_N(T_b;\Delta t,Z)$; namely,

$$\underset{\sim}{x}_N(T_b;\underset{\sim}{x}_0^*) - \underset{\sim}{X}(\Delta t,Z;\underset{\sim}{x}_0^*)\ \underset{\sim}{\alpha}(T_b;\Delta t,Z,N) = -\underset{\sim}{\varepsilon}_N(T_b;\Delta t,Z) \tag{2.33}$$

Observe that $\underset{\sim}{\varepsilon}_N(T_b;\Delta t,Z) \to \underset{\sim}{0}$ if the following 3 conditions are satisfied:

1) $Z = \infty$.
2) $\underset{\sim}{x}_{ss}(t)$ is calculated by solving (1.1) numerically with $\underset{\sim}{x}_0^*$ as the initial state, where $\underset{\sim}{x}_0^*$ is any initial state which satisfies (1.18).
3) $\underset{\sim}{x}_{ss}(t)$ is calculated with infinite precision and zero local truncation error.

None of these conditions can be exactly met in practice. Moreover, even if $\underset{\sim}{\varepsilon}_N(T_b;\Delta t,Z) = \underset{\sim}{0}$, we still can not solve (2.33) for $\underset{\sim}{x}_0^*$ since we do not as yet have the information (i.e., the coefficients $\underset{\sim}{a}_0,\underset{\sim}{a}_1,\underset{\sim}{a}_2,\ldots\underset{\sim}{a}_{2N}$) needed in (2.3) to calculate $\underset{\sim}{x}_N(T_b;\underset{\sim}{x}_0^*)$.

Instead of (2.33), however, suppose we define the following system of "n" related equations as a function of the "n" components $x_{0_1},x_{0_2},\ldots,x_{0_n}$ of the initial vector $\underset{\sim}{x}_0 \triangleq [x_{0_1}\ x_{0_2}\ \ldots\ x_{0_n}]^T = [x_1(0)\ x_2(0)\ \ldots\ x_n(0)]^T$:

$$\underbrace{\begin{bmatrix} x_1(T_b;\underset{\sim}{x}_0) \\ x_2(T_b;\underset{\sim}{x}_0) \\ \vdots \\ x_n(T_b;\underset{\sim}{x}_0) \end{bmatrix}}_{\underset{\sim}{x}(T_b;\underset{\sim}{x}_0)} - \underbrace{\begin{bmatrix} x_{0_1} & x_1(\Delta t;\underset{\sim}{x}_0) & x_1(2\Delta t;\underset{\sim}{x}_0)\ldots x_1(Z\Delta t;\underset{\sim}{x}_0) \\ x_{0_2} & x_2(\Delta t;\underset{\sim}{x}_0) & x_2(2\Delta t;\underset{\sim}{x}_0)\ldots x_2(Z\Delta t;\underset{\sim}{x}_0) \\ \vdots & \vdots & \\ x_{0_n} & x_n(\Delta t;\underset{\sim}{x}_0) & x_n(2\Delta t;\underset{\sim}{x}_0)\ldots x_n(Z\Delta t;\underset{\sim}{x}_0) \end{bmatrix}}_{\underset{\sim}{X}(\Delta t,Z;\underset{\sim}{x}_0)} \underbrace{\begin{bmatrix} \alpha_0(T_b;\Delta t,Z,N) \\ \alpha_1(T_b;\Delta t,Z,N) \\ \alpha_2(T_b;\Delta t,Z,N) \\ \vdots \\ \alpha_Z(T_b;\Delta t,Z,N) \end{bmatrix}}_{\underset{\sim}{\alpha}(T_b;\Delta t,Z,N)} = \begin{bmatrix} 0 \\ 0 \\ \vdots \\ 0 \end{bmatrix}$$

$$\underbrace{\qquad\qquad\qquad\qquad\qquad\qquad\qquad\qquad\qquad\qquad}_{\underset{\sim}{F}(\underset{\sim}{x}_0;T_b,\Delta t,Z,N)} = \underset{\sim}{0} \tag{2.34}$$

where $x_i(t;\underset{\sim}{x}_0)$ denotes the ith component of the complete solution $\underset{\sim}{x}(t) = \underset{\sim}{x}_{tr}(t) + \underset{\sim}{x}_{ss}(t)$ of (1.1) starting from the initial state $\underset{\sim}{x}_0$, for $t = 0, \Delta t, 2\Delta t, \ldots, Z\Delta t$, and T_b. Observe that unlike (2.31), both $\underset{\sim}{x}(T_b;\underset{\sim}{x}_0)$ and $\underset{\sim}{X}(\Delta t,Z;\underset{\sim}{x}_0)$ can be calculated by solving (1.1) numerically.

Now at $\underset{\sim}{x}_0 = \underset{\sim}{x}_0^*$, $\underset{\sim}{x}_{tr}(t) = \underset{\sim}{0}$ for $t \geq 0$ (by definition) and hence we can write

$$\underset{\sim}{x}(T_b;\underset{\sim}{x}_0^*) = \underset{\sim}{x}_{ss}(T_b;\underset{\sim}{x}_0^*) = \underset{\sim}{x}_N(T_b;\underset{\sim}{x}_0^*) + \underset{\sim}{x}_{M-N}(T_b;\underset{\sim}{x}_0^*) \tag{2.35}$$

where $\underset{\sim}{x}_{ss}(T_b;\underset{\sim}{x}_0^*) = \underset{\sim}{x}_{ss}(T_b)$ and $\underset{\sim}{x}_{N*}(T_b;\underset{\sim}{x}_0^*) = \underset{\sim}{x}_N(T_b)$ as defined in (2.1) and (2.3) respectively; and where $\underset{\sim}{x}_{M-N}(T_b;\underset{\sim}{x}_0)$ denotes the remaining (M-N) terms of $\underset{\sim}{x}_{ss}(T_b)$ which have been excluded from $\underset{\sim}{x}_N(T_b)$. Consequently, at $\underset{\sim}{x}_0 = \underset{\sim}{x}_0^*$, (2.34) can be written as follows:

$$\underset{\sim}{x}_N(T_b;\underset{\sim}{x}_0^*) - \underset{\sim}{X}(\Delta t,Z;\underset{\sim}{x}_0^*)\underset{\sim}{\alpha}(T_b;\Delta t,Z,N) = -\underset{\sim}{x}_{M-N}(T_b;\underset{\sim}{x}_0^*) \tag{2.36}$$

Comparing (2.33) and (2.36), we find

$$\boxed{\underset{\sim}{\varepsilon}_N(T_b;\Delta t,Z) = \underset{\sim}{x}_{M-N}(T_b;\underset{\sim}{x}_0^*)} \tag{2.37}$$

Equation (2.37) is remarkable because it says that $\underset{\sim}{\varepsilon}_N(T_b;\Delta t,Z) \to \underset{\sim}{0}$ when $N \to M$. In other words, if the exact steady state response $\underset{\sim}{x}_{ss}(t)$ in (2.1) has only $M < \infty$ frequency components, and if we choose $N = M$ in (2.3), then $\underset{\sim}{\varepsilon}_N(T_b;\Delta t,Z) = \underset{\sim}{0}$ and (2.31) becomes exact for any Z.

Indeed, when M = N and Z = 2M + 1, $\underset{\sim}{\Gamma}$ becomes a square matrix and the generalized Fourier coefficients can be calculated exactly from (2.27):

$$\underset{\sim}{a} = \underset{\sim}{\Gamma}^{-1}\underset{\sim}{x}_{ss}(Z) \tag{2.38}$$

Similarly, (2.32) in this case (Z=2M+1) reduces to

$$\underset{\sim}{\alpha}(T_b;\Delta t,Z) = \underset{\sim}{\Gamma}^T\underset{\sim}{\gamma}(T_b) \tag{2.39}$$

Of course in practice, we will normally choose $N << M$ in order to save computation time. This choice is often necessary anyway because $M = \infty$ for most practical circuits. Fortunately, the amplitudes of the higher-order terms [5] in many practical circuits satisfy (2.2) so that the error vector $\underset{\sim}{\varepsilon}(T_b;\Delta t,Z)$ remains relatively small even though $N << M$.

Let us summarize the preceding observations as follow:

Remarks:

1. The solution $\hat{\underset{\sim}{x}}_0$ of the nonlinear equation

$$\underset{\sim}{F}(\underset{\sim}{x}_0;T_b,\Delta t,Z,N) = \underset{\sim}{0} \tag{2.40}$$

as defined in (2.34) for fixed Δt and Z represents, a good approximation to $\underset{\sim}{x}_0^*$ provided the number of frequency components N and/or the number of time-step samples Z are chosen to be sufficiently large. In particular,

$$\hat{x}_0 \to x_0^* \text{ as } N \to \infty \text{ and/or } Z \to \infty \tag{2.41}$$

2. Since (2.40) is not given in closed analytical form, it must be caluclated numerically for each x_0, Δt, and Z.

3. Equation (2.40) can be solved for x_0 (for fixed Δt and Z) by the Newton-Raphson method [3]:

$$x_0^{(j+1)} = x_0^{(j)} - [J_F(x_0^{(j)})]^{-1} F(x_0^{(j)}; T_b, \Delta t, Z, N) \tag{2.42}$$

$$\text{where } J_F(x_0^{(j)}) \triangleq \left. \frac{\partial F(x_0; T_b, \Delta t, Z, N)}{\partial x_0} \right|_{x_0 = x_0^{(j)}} \tag{2.43}$$

denotes the Jacobian matrix of $F(x_0; T_b, \Delta t, Z, N)$ at $x_0 = x_0^{(j)}$. This can be evaluated by the method given in Section II-C.

4. Once the initial state x_0^* is found, we solve (1.1) numerically with x_0^* as the initial state to obtain $x_{ss}(\Delta t)$, $x_{ss}(2\Delta t), \ldots, x_{ss}(Z\Delta t)$. Substituting the ith component, i = 1,2,...,n, of these data into (2.27), we obtain the first (2N+1) generalized Fourier coeeficients $a_{0_i}, a_{1_i}, \ldots, a_{2N_i}$ of the ith component $x_{ss_i}(t)$ of the steady state response $x_{ss}(t)$.† The steady-state response $x_N(t)$ at any time $t = T_j$ can now be obtained by calculating (2.3) at $t = T_j$.

C. Evaluating the Jacobian matrix $J_F(x_0^{(j)})$

Since the most time-consuming part in solving for x_0 via the Newton-Raphson method is the numerical calculation of the Jacobian matrix $J_F(x_0^{(j)})$, it is essential to develop efficient computational methods. Taking the Jacobian of $F(x_0; \Delta t, Z, N)$ in (2.34), we obtain

$$\boxed{J_F(x_0^{(j)}) = \left. \frac{\partial x(T_b; x_0)}{\partial x_0} \right|_{x_0 = x_0^{(j)}} - \sum_{k=0}^{Z} \alpha_k(T_b; \Delta t, Z) \left. \frac{\partial x(k\Delta t; x_0)}{\partial x_0} \right|_{x_0 = x_0^{(j)}}} \tag{2.44}$$

Hence, we need to calculate

$$\left. \frac{\partial x(t; x_0)}{\partial x_0} \right|_{x_0 = x_0^{(j)}} \text{ at } t = 0, \Delta t, 2\Delta t, \ldots, Z\Delta t, \text{ and } T_b \tag{2.45}$$

These (Z+2) n x n matrices can be calculated by the numerical differentiation method described in Section 17-5-2 of [3]. If the circuit associated with (1.1)

† If $x_{ss}(t)$ is periodic and its period T is not too large, we can replace this step by numerically solving (1.1) from t = 0 to t = T with x_0^* as the initial state.

is given, the most efficient method for calculating (2.45) is the sensitivity network approach given in Section 17-5-3 of [3].

However, if (1.1) is available only analytically†, the sensitivity network approach is not applicable. In this case, the following method is much more efficient and accurate than that of numerical differentiation:

In vector form, (1.1) becomes

$$\underset{\sim}{f}(\dot{\underset{\sim}{x}},\underset{\sim}{x},\underset{\sim}{y};\omega_1 t,\omega_2 t,\ldots,\omega_p t) = \underset{\sim}{0} \tag{2.46}$$

Applying Taylor Expansion about $(\underset{\sim}{x}^{(j)}(t),\underset{\sim}{y}^{(j)}(t))$ at the jth stage of the iteration, where $(\underset{\sim}{x}^{(j)}(t),\underset{\sim}{y}^{(j)}(t))$ denotes the solution of (2.41) with initial state $\underset{\sim}{x}_0 = \underset{\sim}{x}_0^{(j)}$, we obtain

$$\underset{\sim}{f}(\dot{\underset{\sim}{x}}^{(j)}(t),\underset{\sim}{x}^{(j)}(t),\underset{\sim}{y}^{(j)}(t),\omega_1 t,\omega_2 t,\ldots,\omega_p t) + \begin{bmatrix} \frac{\partial \underset{\sim}{f}}{\partial \dot{\underset{\sim}{x}}} & \frac{\partial \underset{\sim}{f}}{\partial \underset{\sim}{x}} & \frac{\partial \underset{\sim}{f}}{\partial \underset{\sim}{y}} \end{bmatrix} \begin{bmatrix} \dot{\underset{\sim}{\eta}}(t) \\ \underset{\sim}{\eta}(t) \\ \underset{\sim}{\gamma}(t) \end{bmatrix}$$

$$+ \underset{\sim}{0}(\|\dot{\underset{\sim}{\eta}}(t)\|^2,\|\underset{\sim}{\eta}(t)\|^2,\|\underset{\sim}{\gamma}(t)\|^2) = \underset{\sim}{0} \tag{2.47}$$

where

$$\underset{\sim}{\eta}(t) \triangleq \underset{\sim}{x}(t) - \underset{\sim}{x}^{(j)}(t),\ \underset{\sim}{\gamma}(t) \triangleq \underset{\sim}{y}(t) - \underset{\sim}{y}^{(j)}(t) \tag{2.48}$$

The first term in (2.47) is identically zero because $(\underset{\sim}{x}^{(j)}(t),\underset{\sim}{y}^{(j)}(t))$ is a solution of (2.46). Neglecting the higher-order terms, (2.47) can be recast as follow:

$$\begin{bmatrix} \dot{\underset{\sim}{\eta}}(t) \\ \underset{\sim}{\gamma}(t) \end{bmatrix} = - \begin{bmatrix} \frac{\partial \underset{\sim}{f}}{\partial \dot{\underset{\sim}{x}}} & \frac{\partial \underset{\sim}{f}}{\partial \underset{\sim}{y}} \end{bmatrix}^{-1} \begin{bmatrix} \frac{\partial \underset{\sim}{f}}{\partial \underset{\sim}{x}} \end{bmatrix} \Bigg|_{(\underset{\sim}{x}^{(j)}(t),\underset{\sim}{y}^{(j)}(t))} \underset{\sim}{\eta}(t) \triangleq \begin{bmatrix} \underset{\sim}{A}^{(j)}(t) \\ \underset{\sim}{B}^{(j)}(t) \end{bmatrix} \underset{\sim}{\eta}(t) \tag{2.49}$$

The first component equation of (2.49) is a linear time-varying differential equation

†Our algorithms in this paper are valid for any equation of the form (1.1), which need not be associated with a circuit.

$$\boxed{\dot{\underset{\sim}{\eta}}(t) = \underset{\sim}{A}^{(j)}(t)\ \underset{\sim}{\eta}(t)} \tag{2.50}$$

where $\underset{\sim}{A}^{(j)}(t)$ is an $n \times n$ matrix function of time. We will henceforth refer to (2.50) as the variational equation associated with (2.46).

The solution of (2.50) corresponding to any initial state $\underset{\sim}{\eta}(0)$ is given by [13]

$$\underset{\sim}{\eta}(t) = \underset{\sim}{\Phi}^{(j)}(t)\ \underset{\sim}{\eta}(0) \tag{2.51}$$

where $\underset{\sim}{\Phi}^{(j)}(t)$ is the fundamental matrix solution of (2.50).† If we choose

$$\underset{\sim}{\eta}(0) = [0\ 0\ \ldots\ 0\ \ \eta_k(0)\ \ 0\ 0\ \ldots\ 0]^T \tag{2.52}$$

then

$$\eta_i(t) = \Phi_{ik}^{(j)}(t)\ \eta_k(0),\ j = 1,2,\ldots,n \tag{2.53}$$

where $\Phi_{ik}(t)$ denotes the ikth element of $\underset{\sim}{\Phi}(t)$. It follows from (2.52) that

$$\frac{\partial x_i(t)}{\partial x_k(0)} = \frac{\eta_i(t)}{\eta_k(0)} = \Phi_{ik}(t) \tag{2.54}$$

Hence we have proved that

$$\boxed{\left.\frac{\partial \underset{\sim}{x}(t;x_0)}{\partial \underset{\sim}{x}_0}\right|_{\underset{\sim}{x}_0=\underset{\sim}{x}_0^{(j)}} = \underset{\sim}{\Phi}^{(j)}(t)} \tag{2.55}$$

It follows from (2.54) that $\underset{\sim}{J}_F(\underset{\sim}{x}_0^{(j)})$ in (2.44) can be calculated accurately in 3 steps:

1) Form the variational equation (2.50) at each iteration.
2) Calculate the fundamental matrix solution $\underset{\sim}{\Phi}^{(j)}(t)$ of (2.50).
3) Calculate (2.44).

D. Initialization Guidelines

To initiate the algorithm for finding the initial state $\underset{\sim}{x}_0^*$, it is necessary to choose the 5 parameters N, Z, Δt, T_b and $\underset{\sim}{x}_0$ for constructing the nonlinear equation (2.34). Since a good choice of these parameters depends on both the nature of the problem (number of state variables, degree of nonlinearity, amplitudes of input signals, number of input frequencies, etc.) and the computer being used (word length, single or double precision, etc.), we can only offer

†The jth column of the fundamental matrix solution is simply the solution of (2.51) with the initial state

$$\underset{\sim}{\eta}(0) = [0\ 0\ \ldots\ 0\ 1\ 0\ \ldots\ 0]^T$$
$$\uparrow \text{jth position}$$

some guidelines which have been found useful in our numerous numerical experiments conducted using our algorithm.

a) Choice of N.

Recall $N \leq M$ is the number of frequency components used in the truncated steady state solution $\underset{\sim}{x}_N(t)$ in (2.3). For typical communication circuits (amplifiers, mixers, modulators, etc.) the number of significant frequency components is usually known from previous analysis and N should be chosen to include all such components.

If the number of significant frequency components is not known from previous experience, we simply make an intuitive guess. If this guess is unrealistic, it will show up in the subsequent error analysis (to be discussed in Section II-E) and we will have to repeat the analysis with a larger N.

b) Choice of Z, Δt, and T_b.

Recall that Δt is the uniform sampling step size used in "sampling" the numerical solution of (1.1) and Z is the total number of samples taken. It is important to note that "Δt" is not the same as the integration step size "h" used in solving (1.1).

In most of our numerical experiments, we solve (1.1) using a 4th-6th order BDF algorithm [3] with a step size $h = T_{min}/50$, where T_{min} is the smallest period of the N frequency components. This choice usually gives a very accurate numerical solution for $\underset{\sim}{x}(t)$.

Our sampling step size Δt is usually chosen within the range

$$\boxed{7h < \Delta t < 13h} \tag{2.56}$$

provided (2.21) is satisfied. In practice, ill-conditioning could occur if Δt is chosen to be too small, or if it contains some frequency components ν_j and ν_k such that $|\nu_j - \nu_k| \approx 0$. (See Appendix B)

Although Theorem 3 shows that the generalized Fourier coefficients can be calculated exactly only if $Z \to \infty$ (see Eq. (2.20)), our numerical experiments show that good results can be obtained in many practical cases with a considerably smaller Z. In particular we have found the following range to be adequate for the many examples we have tried so far:

$$\boxed{(2N+1) < Z < 2(2N+1)} \tag{2.57}$$

Finally, the choice of T_b is somewhat arbitrary as it does not affect the theory in Sec. II-A from which our algorithm is based. However, since the generalized Fourier coefficients are estimated by samples taken over the time interval $[0,Z\Delta t]$, we choose

$$\boxed{T_b > Z\Delta t} \tag{2.58}$$

so that the data $\underset{\sim}{x}(T_b;\underset{\sim}{x}_0)$ would not be redundant.

c) Choice of $\underset{\sim}{x}_0$.

To assure and to hasten the convergence of the Newton-Raphson iteration, it is desirable to pick a good initial guess $\underset{\sim}{x}_0^{(0)}$. Unfortunately, no intuitive guidelines are available especially when the steady state solution $\underset{\sim}{x}_{ss}(t)$ is not periodic.

One approach which has worked well for our examples is to replace the input frequencies $\{\nu_1,\nu_2,\ldots,\nu_N\}$ by an approximate set of frequencies $\{\hat{\nu}_1,\hat{\nu}_2,\ldots,\hat{\nu}_N\}$ so that the associated steady-state waveform is periodic with a relatively small period $T = 2\pi(n/m)$, where m and n are defined in (1.8)-(1.9) and is bounded by (1.16). Using this approximate set of frequencies, we then apply the shooting method [11], or any other efficient method for finding $\underset{\sim}{x}_0^*$ for periodic solutions, to calculate $\underset{\sim}{x}_0^*$. We then take this approximate $\underset{\sim}{x}_0^*$ as our initial guess $\underset{\sim}{x}_0^{(0)}$.

If we let $m_{max} \triangleq \max\{m_1,m_2,\ldots,m_N\}$ and $n_{min} \triangleq \min\{n_1,n_2,\ldots,n_N\}$, then (1.7) suggests the following algorithm for reducing T:

(1) If $\nu_k = m_k$ is an integer for all $k = 1,2,\ldots,N$, then we increase m_{max} until it is not a prime number and then increase ν_k, $k = 1,2,\ldots,N$, until $\hat{m}_{max}/\nu_k$ is an integer.

Example 1. Let $\nu_1 = 2$, $\nu_2 = 3$, and $\nu_3 = 7$. Then $\{m_1,m_2,m_3\} = \{2,3,7\}$ and we have from (1.7)

$$T = \frac{2\pi}{\text{G.C.D.}\{2,3,7\}} = 2\pi$$

Now increase $m_{max} = 7$ to $\hat{\nu}_3 = \hat{m}_3 = 8$, and then increase ν_2 to 4. The new period associated with $\{\hat{\nu}_1,\hat{\nu}_2,\hat{\nu}_3\} = \{2,4,8\}$ is

$$\hat{T} = \frac{2\pi}{\text{G.C.D.}\{2,4,8\}} = \pi \tag{2.59}$$

(2) If $\nu_k = m_k/n_k$ is not an integer, we first change m_k as in (1) and then change n_k, $k = 1,2,\ldots,N$ until it becomes a multiple of n_{min}.

Example 2. Let $\nu_1 = 2/5$, $\nu_2 = 3/8$, and $\nu_3 = 7/9$. Then $\{m_1,m_2,m_3\} = \{2,3,7\}$ as in Example 1 and $\{n_1,n_2,n_3\} = \{5,8,9\}$. From (1.7), we find

$$T = 2\pi \left[\frac{\text{L.C.M.}\{5,8,9\}}{\text{G.C.D.}\{2,3,7\}} \right] = 720\pi \tag{2.60}$$

Since $n_{min} = 5$, we change n_2 and n_3 to $\hat{n}_2 = 10$, and $\hat{n}_3 = 10$ so that

$$\hat{T} = 2\pi \left[\frac{\text{L.C.M.}\{5,10,10\}}{\text{G.C.D.}\{2,4,8\}} \right] = 10\pi \tag{2.61}$$

Note that dramatic reduction in period from 720π to 10π![†]

(3) If ν_k is an irrational number, we first approximate it by a rational number and then proceed as in (2).

Example 3. Let $\nu_1 = 0.404040\ldots$, $\nu_2 = 0.375010101\ldots$, and $\nu_3 = 0.7777\ldots$. We can approximate ν_1, ν_2, and ν_3 by $\hat{\nu}_1 = 2/5$, $\hat{\nu}_2 = 3/8$, and $\hat{\nu}_3 = 7/9$ and then proceed as in Example 2. Note the period changes from $T = \infty$ to $T = 10\pi$.

E. Termination Guidelines

Since our choice of N may not be realistic in the sense that one or more significant frequency components may have been inadvertently excluded from (2.3), our algorithm does not terminate when the Newton-Raphson iteration in (2.42) converges to an initial state $\underset{\sim}{x}_0^*$. We must further validate our answer as follows:

(1) If the steady-state response $\underset{\sim}{x}_{ss}(t)$ is periodic with a reasonably small period T, we simply solve (1.1) numerically for $\underset{\sim}{x}(t,\underset{\sim}{x}_0^*)$ (with $\underset{\sim}{x}_0^*$ as initial state) from t = 0 to t = T and verify that $\underset{\sim}{x}(0;\underset{\sim}{x}_0) \cong \underset{\sim}{x}(T;\underset{\sim}{x}_0)$

(2) If the steady-state response $\underset{\sim}{x}_{ss}(t)$ is not periodic, or if it is periodic with an unreasonably large period T, we can carry out the following heuristic validation procedure in view of (2.7) of Theorem 2.

(a) Solve (1.1) numerically for $\underset{\sim}{x}(t,\underset{\sim}{x}_0^*)$ (with $\underset{\sim}{x}_0^*$ as initial state) from t = 0 to t = T, where T is chosen to be sufficiently large.

(b) Solve for $\underset{\sim}{x}_N(k\Delta t,\underset{\sim}{x}_0^*)$ using (2.31) where $T_b = k\Delta t$ and the entries $x_{ss_j}(k\Delta t)$ in the matrix $\underset{\sim}{X}(\Delta t,Z;\underset{\sim}{x}_0^*)$ are substituted by $x_j(t;\underset{\sim}{x}_0^*)$, t = 0, Δt, $2\Delta t$,...$Z\Delta t$.

(c) Calculate the error

$$\varepsilon_j \triangleq \sqrt{\frac{1}{T}\left\{ \sum_{k=0}^{Z} [x_j(k\Delta t;\underset{\sim}{x}_0^*) - x_{N_j}(k\Delta t;\underset{\sim}{x}_0^*)]^2 \right\}} \tag{2.62}$$

[†]We could reduce $\hat{T}$ further by decreasing (instead of increasing) n_2 and n_3 to $\hat{n}_2 = 5$ and $\hat{n}_3 = 5$. However, the ν_2 and ν_3 no longer represent a good approximation.

for each component $j = 1,2,\ldots,n$.

If $\max\{\varepsilon_1,\varepsilon_2,\ldots,\varepsilon_n\}$ is smaller than some perscribed tolerance, stop. Otherwise, increase N and/or Z and start all over again.

F. Summary of Multi-Frequency Algorithm

Step 0. Specify the 4 parameters N, Z, Δt, and T_b (See Section II-D) and calculate the vector $\underset{\sim}{\alpha}(T_b;\Delta t,Z,N)$ using (2.32).
Set $j = 0$.

Step 1. Choose initial state $\underset{\sim}{x}_0 = \underset{\sim}{x}_0^{(j)}$ (for $j = 0$, see Section II-D) and solve (1.1) numerically to obtain $\underset{\sim}{x}(\Delta t),\underset{\sim}{x}(2\Delta t),\ldots,\underset{\sim}{x}(Z\Delta t)$.
Calculate $\underset{\sim}{F}(\underset{\sim}{x}_0;T_b,\Delta t,Z,N)$ from (2.34). If $\|\underset{\sim}{F}(\underset{\sim}{x}_0;T,\Delta t,Z,N)\| < \varepsilon$ whose ε is a sufficiently small positive number, call $\underset{\sim}{x}_0 = \underset{\sim}{x}_0^*$ and go to Step 4.

Step 2. Compute the Jacobian matrix $\underset{\sim}{J}_F(\underset{\sim}{x}_0^{(j)})$ in (2.43). (See Section II-C).

Step 3. Compute $\underset{\sim}{x}_0^{(j+1)}$ via the Newton-Raphson iteration (2.42).
Go to Step 1 with $j \to j + 1$.

Step 4. Solve (1.1) for $\underset{\sim}{x}(t)$ with $\underset{\sim}{x}_0^*$ as initial state from $t = 0$ to $t = T_b$ where T_b = period if $\underset{\sim}{x}_{ss}(t)$ is periodic, or T_b is a sufficiently large number.

Case 1. $\underset{\sim}{x}_{ss}(t)$ is periodic with small period T:
Calculate $\varepsilon_j = x_j(0,\underset{\sim}{x}_0^*) - x_j(T;\underset{\sim}{x}_0^*)$, $j = 1,2,\ldots,n$

Case 2. $\underset{\sim}{x}_{ss}(t)$ is not periodic or is periodic with large T:
Calculate ε_j using (2.62), $j = 1,2,\ldots,n$.

If $\max\{\varepsilon_1,\varepsilon_2,\ldots,\varepsilon_n\} > \varepsilon_0$
where ε_0 is a sufficiently small positive number, increase N and/or Z and repeat Steps 0-4.

Step 5. STOP.

G. Illustrative Examples

Numerous examples have been solved successfully using the 2 algorithms presented in Sections II and III. Because of its widespread interest, let us apply the preceding algorithm to solve the forced Duffing's equation [14-15]:

$$\ddot{x} + k\dot{x} + c_1x + c_2x^3 = f(t) \tag{2.63}$$

This equation arises in many physical problems (e.g., ferro-resonance circuits) and is known to exhibit many interesting phenomena; including subharmonic, almost-

periodic, and chaotic solutions [16].

To apply our algorithm, let us recast (2.63) into the form of (1.1), which in this case is just the state equation

$$\boxed{\begin{aligned}\dot{x}_1 &= x_2 \\ \dot{x}_2 &= -kx_2 - c_1x_1 - c_2x_1^3 + f(t)\end{aligned}} \tag{2.64}$$

To be specific, let us choose a 3-frequency-input signal

$$f(t) = A_1 \cos \omega_1 t + A_2 \cos \omega_2 t + A_3 \cos \omega_3 t \tag{2.65}$$

and $k = 0.1$, $c_1 = 2.0$ and $c_2 = 1.0$.

We have solved (2.64) using many different combinations of amplitudes and frequencies, 4 of which are listed in Table 2.

Table 2. Four combinations of A_i and ω_i and their respective periods.

case	A_1	A_2	A_3	ω_1	ω_2	ω_3	$T_1 = \frac{2\pi}{\omega_1}$	$T_2 = \frac{2\pi}{\omega_2}$	$T_3 = \frac{2\pi}{\omega_3}$	$T = 2\pi(\frac{n}{m})$
1	0.4	0.4	0.4	1	0.35	0.155	6.283	17.951	40.54	400π
2	0.4	0.4	0.4	1	0.85	0.170	6.283	7.392	36.96	200π
3	0.5	0.5	0.5	1	0.35	0.155	6.283	17.951	40.53	400π
4	0.5	0.5	0.5	1	0.85	0.170	6.283	7.392	36.96	200π

From previous experience, we know all frequency components

$$\nu_k = m_{1k}\omega_1 + m_{2k}\omega_2 + m_{3k}\omega_3 \tag{2.65}$$

with

$$|m_{1k}| + |m_{2k}| + |m_{3k}| \leq 3 \tag{2.66}$$

are likely to be non-negligible. Since these are 30 frequency components satisfying (2.66), we choose $N = 30$ in (2.3). Applying the preceding algorithm with $\Delta t = 11\ T_1/50$, $Z = 1.5(60) = 90$, and $T_b = 23\ T_1$, we obtain the initial state $\underset{\sim}{x}_0^*$ listed in Table 3 corresponding to the 4 cases in Table 2. Also listed is the error ε_j calculated using (2.62)

Table 3. Initial state computed using multi-frequency algorithm with a 6th order BDF algorithm [3].

case	$\underset{\sim}{x}_0^* \triangleq \underset{\sim}{x}^*(0)$		Error	
	$x_1^*(0)$	$x_2^*(0)$	ε_1	ε_2
1	0.69667	-0.18304	$0.53(10^{-3})$	$0.99(10^{-3})$
2	0.78298	-0.13834	$0.14(10^{-2})$	$0.22(10^{-2})$
3	0.82931	-0.32269	$0.92(10^{-3})$	$0.14(10^{-2})$
4	0.81562	-0.46932	$0.33(10^{-2})$	$0.57(10^{-2})$

Using the initial states from Table 3 and (2.27), we have calculated the 60 generalized Fourier coefficients $a_1, a_2, \ldots, a_{60}$ in (2.3) corresponding to N = 30 for cases 1 and 2. The waveforms of $x_1(t)$ for these 2 cases are plotted (using (2.3)) as the solid waveforms in Figs. 1(a) and 2(a), respectively. As a check over the accuracy of our solutions, we solve (1.1) using the same initial states and the solution at each integration time step is shown as "dots" in Figs. 1(a) and 2(a) respectively. Note the remarkable accuracy in both cases.

To compare the amplitudes of the 30 frequency components, we use (2.27) to plot the discrete frequency spectrum for these 2 cases in Figs. 1(b) and 2(b), respectively.

Finally, to obtain a measure of the rate of convergence of the Newton-Raphson iteration (2.42), the error

$$\varepsilon^{(j)} \triangleq \sqrt{F_1^2(\underset{\sim}{x}_0^{(j)};T_b,\Delta t,Z,N)+F_2^2(\underset{\sim}{x}_0^{(j)};T_b,\Delta t,Z,N)} \tag{2.67}$$

at each iteration is plotted in Fig. 3 for cases 1 and 2, respectively. Note that both converges rapidly in 4 iterations.

III. Almost-Periodic Solution Algorithm 2: Two Input Frequencies

In this section, we assume the circuit or system is driven by no more than 2 frequencies; i.e., $P \leq 2$ in (1.1). Hence, let us rewrite (1.1) and (1.5) as follows:

$$\underset{\sim}{f}(\dot{\underset{\sim}{x}},\underset{\sim}{x},\underset{\sim}{y};\omega_1 t,\omega_2 t) = \underset{\sim}{0} \tag{3.1}$$

$$\nu_k = m_{1k}\omega_1 + m_{2k}\omega_2,\ k = 1,2,\ldots,M \tag{3.2}$$

Substituting (3.2) into (1.4) and making use of standard trigonometric identities, we can recast the steady-state response $\underset{\sim}{x}_{ss}(t)$ as follow:

$$\begin{aligned}
\underset{\sim}{x}_{ss}(t) &= \underset{\sim}{a}_0 + \sum_{k=1}^{M} \left\{ \underset{\sim}{a}_{2k-1} \cos(m_{1k}\omega_1+m_{2k}\omega_2)t + \underset{\sim}{a}_{2k} \sin(m_{1k}\omega_1+m_{2k}\omega_2)t \right\} \\
&= \underset{\sim}{a}_0 + \sum_{k=1}^{M} \left\{ \underset{\sim}{a}_{2k-1} [(\cos m_{1k}\omega_1 t)(\cos m_{2k}\omega_2 t)-(\sin m_{1k}\omega_1 t)(\sin m_{2k}\omega_2 t)] \right. \\
&\qquad \left. + \underset{\sim}{a}_{2k}[(\sin m_{1k}\omega_1 t)(\cos m_{2k}\omega_2 t)+(\cos m_{1k}\omega_1 t)(\sin m_{2k}\omega_2 t)] \right\} \\
&= \underset{\sim}{a}_0 + \sum_{k=1}^{M} \left\{ [\underset{\sim}{a}_{2k-1} \cos m_{1k}\omega_1 t+\underset{\sim}{a}_{2k} \sin m_{1k}\omega_1 t] \cos m_{2k}\omega_2 t \right. \\
&\qquad \left. + [\underset{\sim}{a}_{2k} \cos m_{1k}\omega_1 t-\underset{\sim}{a}_{2k-1} \sin m_{1k}\omega_1 t] \sin m_{2k}\omega_2 t \right\} \qquad (3.3)
\end{aligned}$$

If we let B denote an integer bound such that

$$|m_{1k}| + |m_{2k}| \leq B \qquad (3.4)$$

then the number M of non-zero frequency components ν_k is given in Table 4 for B = 1,2,...,10.

Table 4. The integers M, 2M + 1, and 2B + 1 as a function of B.

B	1	2	3	4	5	6	7	8	9	10
M	2	6	12	20	30	42	56	72	90	110
2M+1	5	13	25	41	61	85	113	145	181	221
2B+1	3	5	7	9	11	13	15	17	19	21

This table can be easily verified by counting the number of solid dots subtended by an isosceles triangle of base length 2B in Fig. 4. For example, we can enumerate the following frequency components when B = 3:

$\nu_1 = \omega_1$, $\nu_2 = \omega_2$, $\nu_3 = 2\omega_1$, $\nu_4 = 2\omega_2$, $\nu_5 = 3\omega_1$, $\nu_6 = 3\omega_2$, $\nu_7 = \omega_1 + \omega_2$, $\nu_8 = \omega_1 - \omega_2$, $\nu_9 = \omega_1 + 2\omega_2$, $\nu_{10} = \omega_1 - 2\omega_2$, $\nu_{11} = 2\omega_1 + \omega_2$, and $\nu_{12} = 2\omega_1 - \omega_2$. Hence, M(3) = 12.

Observe that all solid dots on the m_{1k}-axis in Fig. 4 denote harmonics of ω_1. Likewise, those on the m_{2k}-axis denote harmonics of ω_2. All other solid dots

denote intermodulation components. In particular, all solid dots on a horizontal line through $m_{2k} = N$, $N = 1,2,\ldots$, correspond to frequency components of the form $\nu_k = m_{1k}\omega_1 + N\omega_2$. Hence, if we regroup all frequency components in (3.3) corresponding to dots on a horizontal line together, we can recast (3.3) into the form

$$\boxed{\underset{\sim}{x}_{ss}(t) = \underset{\sim}{g}_0(t) + \sum_{k=1}^{B} \{ \underset{\sim}{g}_{2k-1}(t) \cos k\omega_2 t + \underset{\sim}{g}_{2k}(t) \sin k\omega_2 t\}} \tag{3.5}$$

where $\underset{\sim}{g}_0(t)$, $\underset{\sim}{g}_1(t)$, $\underset{\sim}{g}_2(t),\ldots,\underset{\sim}{g}_{2B}(t)$ contain only cosine and since components which are harmonics of ω_1 and are therefore all <u>periodic</u> functions of period $T_1 = 2\pi/\omega_1$. Since this observation is the basis of <u>Algorithm 2</u>, we will restate it as a theorem:

<u>Theorem 4</u>.

The steady-state response $\underset{\sim}{x}_{ss}(t)$ in (3.3) which contains (2M+1) generalized Fourier coefficients can be recast into the form of (3.5) containing only (2B+1) <u>coefficient functions of time</u> $\underset{\sim}{g}_0(t)$, $\underset{\sim}{g}_1(t)$, $\underset{\sim}{g}_2(t),\ldots,\underset{\sim}{g}_{2B}(t)$ which are all <u>periodic</u> of period $T_1 = 2\pi/\omega_1$.

A comparison between the number of coefficients describing (3.3) and (3.5) is given in <u>Table 4</u>. Observe that (3.5) has <u>much fewer</u> coefficients compared to that of (3.3) specially for large B. For example, when B = 8, <u>Algorithm 1</u> from <u>Section II</u> would entail solving for 145 generalized Fourier coefficients, whereas only 17 coefficient functions need be specified in (3.5). Our objective in this section is to develop a new algorithm which takes full advantage of this remarkably concise form of solution.

A. <u>Calculating $\underset{\sim}{g}_k(0)$ when transient component is zero</u>.

In <u>Section III-B</u>, we will present an algorithm for finding an initial state $\underset{\sim}{x}_0^*$ such that the transient component $\underset{\sim}{x}_{tr}(t)$ in (1.3) is zero for $t \geq 0$. In this subsection, let us assume $\underset{\sim}{x}_0^*$ has been found so that the solution of (3.1) starting from $\underset{\sim}{x}_0^*$ is $\underset{\sim}{x}(t) = \underset{\sim}{x}_{ss}(t)$ for $t \geq 0$, where $\underset{\sim}{x}_{ss}(t)$ is given by (3.5).

For reasons that will be clear in <u>Section III-B</u>, we need to derive a relationship for calculating $\underset{\sim}{g}_k(0)$, $k = 0,1,2,\ldots,2B$, in terms of "(2B+1)" samples $\underset{\sim}{x}_{ss}(0)$, $\underset{\sim}{x}_{ss}(T_1)$, $\underset{\sim}{x}_{ss}(2T_1),\ldots,\underset{\sim}{x}_{ss}(2BT_1)$ taken at $T_1 = 2\pi/\omega_1$ intervals. Since each component $x_{ss_i}(t)$ of $\underset{\sim}{x}_{ss}(t)$, $i = 1,2,\ldots,n$, can be calculated separately, it suffices for us to derive the <u>i</u>th component $g_{i,k}(0)$ of $\underset{\sim}{g}_k(0)$.

Substituting $t = 0, T_1, 2T_1, \ldots, 2BT_1$ into (3.5)

and using

$$g_{i,k}(kT_1) = g_{i,k}(0), \quad k = 1,2,\ldots,2B \tag{3.6}$$

in view of <u>Theorem 4</u>, we obtain

$$\left.\begin{aligned}
x_{ss_i}(0) &= g_{i,0}(0) + \sum_{k=1}^{B} g_{i,2k-1}(0) \\
x_{ss_i}(T_1) &= g_{i,0}(0) + \sum_{k=1}^{B} \left\{ g_{i,2k-1}(0) \cos k\omega_2 T_1 + g_{i,2k}(0) \sin k\omega_2 T_1 \right\} \\
x_{ss_i}(2T_1) &= g_{i,0}(0) + \sum_{k=1}^{B} \left\{ g_{i,2k-1}(0) \cos 2k\omega_2 T_1 + g_{i,2k}(0) \sin 2k\omega_2 T_1 \right\} \\
&\vdots \qquad\qquad \vdots \qquad\qquad\qquad\qquad \vdots \\
x_{ss_i}(2BT_1) &= g_{i,0}(0) + \sum_{k=1}^{B} \left\{ g_{i,2k-1}(0) \cos 2kB\omega_2 T_1 + g_{i,2k}(0) \sin 2kB\omega_2 T_1 \right\}
\end{aligned}\right\} \quad (3.7)$$

Equation (3.7) consists of 2B+1 equations in terms of the 2B+1 coefficients $g_{i,0}(0), g_{i,1}(0), g_{i,2}(0), \ldots, g_{i,2B}(0)$.

If we define the (2B+1)-vectors

$$\underset{\sim}{x}_{ss_i}(B) \triangleq \begin{bmatrix} x_{ss_i}(0) \\ x_{ss_i}(T_1) \\ x_{ss_i}(2T_1) \\ \vdots \\ x_{ss_i}(2BT_1) \end{bmatrix} \text{ and } \underset{\sim}{g}_{B_i} \triangleq \begin{bmatrix} g_{i,0}(0) \\ g_{i,1}(0) \\ g_{i,2}(0) \\ \vdots \\ g_{i,2B}(0) \end{bmatrix} \quad (3.8)$$

and the (2B+1) × (2B+1) square matrix

$$\underset{\sim}{\Omega}(B) \triangleq \begin{bmatrix} 1 & 1 & 0 & \cdots & 1 & 0 \\ 1 & \cos(\omega_2 T_1) & \sin(\omega_2 T_1) & \cdots & \cos(B\omega_2 T_1) & \sin(B\omega_2 T_1) \\ 1 & \cos(2\omega_2 T_1) & \sin(2\omega_2 T_1) & \cdots & \cos(2B\omega_2 T_1) & \sin(2B\omega_2 T_1) \\ \vdots & \vdots & \vdots & \vdots\vdots\vdots & \vdots & \vdots \\ 1 & \cos(B\omega_2 T_1) & \sin(B\omega_2 T_1) & \cdots & \cos(B^2\omega_2 T_1) & \sin(B^2\omega_2 T_1) \\ \vdots & \vdots & \vdots & \vdots\vdots\vdots & \vdots & \vdots \\ 1 & \cos(2B\omega_2 T_1) & \sin(2B\omega_2 T_1) & \cdots & \cos(2B^2\omega_2 T_1) & \sin(2B^2\omega_2 T_1) \end{bmatrix} \quad (3.9)$$

then (3.7) assumes the condensed form

$$\underset{\sim}{\Omega}(B)\underset{\sim}{g}_{B_i} = \underset{\sim}{x}_{ss_i}(B), \; i = 1,2,\ldots,n \quad (3.10)$$

Theorem 5

The 2B+1 coefficients $g_{i,0}(0), g_{i,1}(0), g_{i,2}(0), \ldots g_{i,2B}(0)$ describing the steady-state response (3.5) can be calculated exactly from

$$\boxed{\underset{\sim}{g}_{B_i} = \underset{\sim}{\Omega}^{-1}(B)\, \underset{\sim}{x}_{ss_i}(B)} \quad , \; i = 1,2,\ldots,n \tag{3.11}$$

The matrix $\underset{\sim}{\Omega}(B)$ is non-singular if, and only if, there does not exist an integer L_2 such that

$$\boxed{\frac{\omega_2}{\omega_1} \neq \frac{L_2}{L_1} \; , \; L_1 = 1,2,\ldots,2B} \tag{3.12}$$

Proof. Eq. (3.11) follows directly from (3.10). The proof that (3.12) is a necessary and sufficient condition for $\underset{\sim}{\Omega}(B)$ to be non-singular is given in Appendix C. ∎

Corollary

1. $\underset{\sim}{\Omega}(B)$ is always non-singular if ω_1 and ω_2 are incommeasurable.
2. If ω_1 and ω_2 are both rational numbers, we can make $\underset{\sim}{\Omega}(B)$ nonsingular by choosing

$$B < \frac{T}{2T_1} \tag{3.13}$$

where T is the period denfined in (1.7).

Proof. Corollary 1 follows directly from (3.12). Corollary 2 is proved in Appendix D.

B. Finding the initial state $\underset{\sim}{x}_0^*$

Consider the ith component of (3.5) at $t = (2B+1)T_1$:

$$x_{ss_i}\left((2B+1)T_1\right) = g_{i,0}(0) + \sum_{k=1}^{Z} \left\{ g_{i,2k-1}(0) \cos(2B+1)\omega_2 T_1 + g_{i,2k}(0) \sin(2B+1)\omega_2 T_1 \right\} \tag{3.14}$$

Substituting (3.11) for $g_{i,k}(0)$ in (3.14), we obtain

$$\begin{aligned} x_{ss_i}\left((2B+1)T_1\right) &= \underset{\sim}{\delta}^T(B)\underset{\sim}{g}_{B_i} = \underset{\sim}{\delta}^T(B)\underset{\sim}{\Omega}^{-1}(B)\underset{\sim}{x}_{ss_i}(B) \\ &= \underset{\sim}{x}_{ss_i}^T(B)\underset{\sim}{\Omega}^{T^{-1}}(B)\underset{\sim}{\delta}(B) \end{aligned} \tag{3.15}$$

where

$$\underset{\sim}{\delta}(B) \triangleq \left[1 \cos[(2B+1)\omega_2 T_1] \sin[(2B+1)\omega_2 T_1] \ldots \cos[(2B+1)B\omega_2 T_1] \sin[(2B+1)B\omega_2 T_1]\right]^T \tag{3.16}$$

Since $[\underset{\sim}{\Omega}^T(B)]^{-1}\ \underset{\sim}{\delta}(B)$ in (3.15) remains unchanged for all i = 1,2,...,n, we can combine all "n" components of $\underset{\sim}{x}_{ss}(t)$ from (3.15) into a single matrix equation:

$$\underbrace{\begin{bmatrix} x_{ss_1}((2B+1)T_1) \\ x_{ss_2}((2B+1)T_1) \\ \vdots \\ x_{ss_n}((2B+1)T_1) \end{bmatrix}}_{\underset{\sim}{x}_{ss}((2B+1)T_1)} = \underbrace{\begin{bmatrix} x_{ss_1}(0) & x_{ss_1}(T_1) & x_{ss_1}(2T_1) & \ldots & x_{ss_1}(2BT_1) \\ x_{ss_2}(0) & x_{ss_2}(T_1) & x_{ss_2}(2T_1) & \ldots & x_{ss_2}(2BT_1) \\ \vdots & \vdots & \vdots & \vdots\vdots & \vdots \\ x_{ss_n}(0) & x_{ss_n}(T_1) & x_{ss_n}(2T_1) & \ldots & x_{ss_n}(2BT_1) \end{bmatrix}}_{\underset{\sim}{X}(B)} \underbrace{\begin{bmatrix} \beta_0(B) \\ \beta_1(B) \\ \beta_2(B) \\ \vdots \\ \beta_{2B}(B) \end{bmatrix}}_{\underset{\sim}{\beta}(B)} \tag{3.17}$$

where the (2B+1) - vector

$$\underset{\sim}{\beta}(B) \triangleq [\underset{\sim}{\Omega}^T(B)]^{-1}\ \underset{\sim}{\delta}(B) \tag{3.18}$$

depends <u>only</u> on B.

Observe that (3.17) is <u>exact</u> provided the integer bound B in (3.4) includes <u>all</u> "M" frequency components of the <u>exact</u> steady-state response $\underset{\sim}{x}_{ss}(t)$ in (3.3). In this case, the entries $\underset{\sim}{x}_{ss}(t)$, $t = 0, T_1, 2T_1, \ldots, 2BT_1$ in $\underset{\sim}{X}(B)$ can be obtained by solving (3.1) using $\underset{\sim}{x}_0^*$ as the initial state.

Since $\underset{\sim}{x}_0^*$ is precisely what we are seeking, let us define the following system of "n" related equations as a function of the "n" components $x_{0_1}, x_{0_2}, \ldots, x_{0_n}$ of the initial vector

$$\underset{\sim}{x}_0 \triangleq [x_{0_1}\ x_{0_2} \ldots x_{0_n}]^T = [x_1(0)\ x_2(0) \ldots x_n(0)]^T:$$

$$\underbrace{\begin{bmatrix} x_1((2B+1)T_1;\underset{\sim}{x}_0) \\ x_2((2B+1)T_1;\underset{\sim}{x}_0) \\ \vdots \\ x_n((2B+1)T_1;\underset{\sim}{x}_0) \end{bmatrix}}_{\underset{\sim}{x}((2B+1)T_1;\underset{\sim}{x}_0)} - \underbrace{\begin{bmatrix} x_1(0) & x_1(T_1;\underset{\sim}{x}_0) & x_1(2T;\underset{\sim}{x}_0) & \cdots & x_1(2BT_1;\underset{\sim}{x}_0) \\ x_2(0) & x_2(T_1;\underset{\sim}{x}_0) & x_2(2T_1;\underset{\sim}{x}_0) & \cdots & x_2(2BT_1;\underset{\sim}{x}_0) \\ \vdots & \vdots & \vdots & \vdots\vdots & \vdots \\ x_n(0) & x_n(T_1;\underset{\sim}{x}_0) & x_n(2T_1;\underset{\sim}{x}_0) & \cdots & x_n(2BT_1;\underset{\sim}{x}_0) \end{bmatrix}}_{\underset{\sim}{X}(B;\underset{\sim}{x}_0)} \underbrace{\begin{bmatrix} \beta_0(B) \\ \beta_1(B) \\ \beta_2(B) \\ \vdots \\ \beta_{2B}(B) \end{bmatrix}}_{\underset{\sim}{\beta}(B)} = \underbrace{\begin{bmatrix} 0 \\ 0 \\ \vdots \\ 0 \end{bmatrix}}_{\underset{\sim}{0}}$$

$$\underbrace{\qquad\qquad\qquad\qquad\qquad\qquad}_{\underset{\sim}{F}(\underset{\sim}{x}_0;B)} \tag{3.19}$$

where

$x_i(kT_1,\underset{\sim}{x}_0)$, k=0,1,...,2B+1 denote the ith component of the complete solution $\underset{\sim}{x}(t) = \underset{\sim}{x}_{tr}(t) + \underset{\sim}{x}_{ss}(t)$ of (3.1) starting from the initial state $\underset{\sim}{x}_0$, for t = 0, $T_1, 2T_1, \ldots 2BT_1, (2B+1)T_1$. Observe that unlike (3.17), both, $\underset{\sim}{x}((2B+1)T_1;\underset{\sim}{x}_0)$ and $\underset{\sim}{X}(B;\underset{\sim}{x}_0)$ can be calculated by solving (3.1) numerically.

Since (3.19) reduces to (3.18) when $\underset{\sim}{x}_0 = \underset{\sim}{x}_0^*$, it follows that $\underset{\sim}{x}_0^*$ can be found by solving

$$\boxed{\underset{\sim}{F}(\underset{\sim}{x}_0;B) = \underset{\sim}{0}} \tag{3.20}$$

by Newton-Raphson iteration as in (2.42), with $\underset{\sim}{F}(\cdot)$ replaced by $\underset{\sim}{F}(\underset{\sim}{x}_0;B)$.

The Jacobian matrix $\underset{\sim}{J}_F(\underset{\sim}{x}_0^{(j)})$ can be evaluated by the sensitivity network approach [3] if the circuit is given. If only the equation (3.1) is given, the Jacobian matrix can be calculated from

$$\boxed{\underset{\sim}{J}_F(\underset{\sim}{x}_0^{(j)}) = \frac{\partial \underset{\sim}{x}((2B+1)T_1;\underset{\sim}{x}_0)}{\partial \underset{\sim}{x}_0}\bigg|_{\underset{\sim}{x}_0=\underset{\sim}{x}_0^{(j)}} - \sum_{k=0}^{2B} \beta_k(B)\, \frac{\partial \underset{\sim}{x}(kT_1;\underset{\sim}{x}_0)}{\partial \underset{\sim}{x}_0}\bigg|_{\underset{\sim}{x}_0=\underset{\sim}{x}_0^{(j)}}} \tag{3.21}$$

where $\dfrac{\partial \underset{\sim}{x}((2B+1)T_1;\underset{\sim}{x}_0)}{\partial \underset{\sim}{x}_0}$ can be evaluated using (2.55).

To save computation time, the integer bound B is chosen to include only the significant frequency components in (3.3). In this case, the initial state $\underset{\sim}{x}_0^*(B)$ computed from (3.20) will depend on B and is therefore not exactly equal to $\underset{\sim}{x}_0^*$. Clearly,

$$\boxed{\underset{\sim}{x}_0^*(B) \to \underset{\sim}{x}_0^* \quad \text{as } B \to B^*} \tag{3.22}$$

where B^* denotes the integer which is large enough to include all frequency components of (3.3).

C. Initialization Guidelines

Since (3.1) must be solved many times numerically from t = 0 to t = $(2B+1)T_1$, we always choose ω_1 to be the larger of the 2 input frequencies. Once ω_1 is identified, we can calculate $\underset{\sim}{F}(\underset{\sim}{x}_0;B)$ in (3.19) by specifying the 2 parameters B and $\underset{\sim}{x}_0$.

a) Choice of B.

The integer bound B in (3.5) should be chosen equal to at least the order of the highest significant harmonics of ω_2 in the steady-state response. It is independent of ω_1. This important property allows us to analyze a large class of communication circuits where the "signal" frequency at ω_2 is much smaller than the "carrier" or "pump" frequency ω_1. In such cases, harmonics of ω_2 will usually be quite small even though the input signal at frequency ω_1 is usually very large (thereby generating many higher harmonics of ω_1) so that accurate answers can often be obtained with B = 3.

If the order of the highest significant harmonics is not known, we simply make an intuitive guess. If this guess is unrealistic, it will reveal itself in the subsequent error analysis (to be discussed in Section III-D).

b) Choice of $\underset{\sim}{x}_0$.

The same procedure presented in Section II-C also applies here.

D. Termination Guidelines.

Recall that in practice, the solution $\underset{\sim}{x}_0^*(B)$ of (3.20) is not the exact solution $\underset{\sim}{x}_0^*$. Consequently, we must validate this answer before terminating.

(1) If the steady-state response $\underset{\sim}{x}_{ss}(t)$ is periodic with a reasonably small period T [see(1.7)] then we simply solve (3.1) numerically for $\underset{\sim}{x}(t;\underset{\sim}{x}_0^*(B))$ (with $\underset{\sim}{x}_0^*(B)$ as initial state) and verify that $\underset{\sim}{x}(0;\underset{\sim}{x}_0^*(B)) \simeq \underset{\sim}{x}(T;\underset{\sim}{x}_0^*(B))$.

(2) If the steady-state response $\underset{\sim}{x}_{ss}(t)$ is not periodic, or if it is periodic with an unreasonably large period T, we can estimate the error with the help of (2.51). If the "approximate" solution $\underset{\sim}{x}(t;\underset{\sim}{x}_0^*(B))$ is indeed close to the exact solution $\underset{\sim}{x}(t;\underset{\sim}{x}_0^*)$ for all $t \geq 0$, then it follows from (2.48) and (2.51) that

$$\|\underset{\sim}{x}(t;\underset{\sim}{x}_0^*) - \underset{\sim}{x}(t;\underset{\sim}{x}_0^*(B))\| \leq \|\underset{\sim}{\Phi}(t)\| \, \|\underset{\sim}{x}_0^* - \underset{\sim}{x}_0^*(B)\| \tag{3.23}$$

for all $t \geq 0$.

If we let $\underset{\sim}{g}_k^*(0)$ and $\underset{\sim}{g}_k(0)$ denote the "exact" (computed using (3.11) with $B = B^*$ and exact $\underset{\sim}{x}_0^*$) and "approximate" (computed using (3.11) with approximate $\underset{\sim}{x}_0^*(B)$) values, then

$$\|\underset{\sim}{x}_0^* - \underset{\sim}{x}_0^*(B)\| = \|[\underset{\sim}{g}_0^*(0)+\sum_{k=1}^{B^*}\underset{\sim}{g}^*_{2k-1}(0)] - [\underset{\sim}{g}_0(0)-\sum_{k=1}^{B}\underset{\sim}{g}_{2k-1}(0)]\|$$

$$\leq \|\underset{\sim}{g}_0^*(0) - \underset{\sim}{g}_0(0)\| + \sum_{k=1}^{B}\|\underset{\sim}{g}^*_{2k-1}(0) - \underset{\sim}{g}_{2k-1}(0)\| + \sum_{k=B+1}^{B^*}\|\underset{\sim}{g}^*_{2k-1}(0)\| \qquad (3.24)$$

Since the coefficients $\underset{\sim}{g}_k^*(0)$ and $\underset{\sim}{g}_k(0)$ can be interpreted as the Fourier coefficients associated with the frequency $k\omega_2$ at $t = 0$, it is reasonable to assume that if $\|\underset{\sim}{g}_k(0)\|$ is sufficiently small for $k > 2B + 1$, the computed initial state $\underset{\sim}{x}_0^*(B)$ will be sufficiently close to $\underset{\sim}{x}_0^*$, and hence

$$\underset{\sim}{g}^*_{2k-1}(0) \simeq \underset{\sim}{g}_{2k-1}(0),\ k = \tfrac{1}{2},1,2,\ldots,B \qquad (3.25)$$

It follows from (3.23), (3.24), and (3.25) that we can <u>approximate</u> (3.23) by

$$\|\underset{\sim}{x}(t;\underset{\sim}{x}_0^*) - \underset{\sim}{x}(t;\underset{\sim}{x}_0^*(B))\| \leq \|\underset{\sim}{\Phi}(t)\|\{\sum_{k=B+1}^{B^*}\|\underset{\sim}{g}^*_{2k-1}(0)\| + \varepsilon(B,\underset{\sim}{x}_0^*(B))\} \qquad (3.26)$$

where $\varepsilon(B,\underset{\sim}{x}_0^*(B))$ is an error from the first two terms in (3.24).

Even though the right hand side of (3.26) can not be calculated from available data, the following <u>heuristic</u> procedure has been used successfully in all examples we have investigated so far:

(1) Solve (3.1) numerically for $\underset{\sim}{x}(t;\underset{\sim}{x}_0^*(B))$ from $t = 0$ to $t = 2(B+2)T_1$.

(2) Calculate $\underset{\sim}{g}_{B_i}$, $i = 1,2,\ldots,n$, using (3.9) and (3.11) with B replaced by B+2 and with $x_{ss_i}(t)$ replaced by $x_i(t;\underset{\sim}{x}_0^*(B))$ for $t = 0,T_1,2T_1,\ldots,2(B+2)T_1$.

(3) If

$$_{B+1}\varepsilon_{B+2} \triangleq \|\underset{\sim}{g}_{2B+1}(0)\| + \|\underset{\sim}{g}_{2B+3}(0)\| \qquad (3.27)$$

is smaller than some prescribed tolerance, <u>stop</u>.
Otherwise, increase B and start all over again.

E. <u>Summary of Two-Frequency Algorithm</u>

<u>Step 0</u>. Choose ω_1 to be the larger of the 2 input frequencies. Specify the integer bound B (<u>see Section III-C</u>). Set $j = 0$.

<u>Step 1</u>. Choose initial state $\underset{\sim}{x}_0 = \underset{\sim}{x}_0^{(j)}$ (for j=0, see <u>Section II-D</u>) and solve (3.1) numerically to obtain $\underset{\sim}{x}(T_1)$, $\underset{\sim}{x}(2T_1)$, $\underset{\sim}{x}(2BT_1)$.
Calculate $\underset{\sim}{F}(\underset{\sim}{x}_0;B)$ from (3.19). If $\|\underset{\sim}{F}(\underset{\sim}{x}_0;B)\| < \varepsilon$, where ε is a sufficiently small positive number, call $\underset{\sim}{x}_0 = \underset{\sim}{x}_0^*(B)$ and go to <u>Step 4.</u>

<u>Step 2</u>. Compute the Jacobian matrix $\underset{\sim}{J}_F(\underset{\sim}{x}_0^{(j)})$ in (3.21) (see <u>Section II-C</u>).

Step 3. Compute $\underset{\sim}{x}_0^{(j+1)}$ via the Newton-Raphson iteration (2.42) with $\underset{\sim}{F}(\cdot)$ replaced by $\underset{\sim}{F}(\underset{\sim}{x}_0,B)$. Go to Step 1 with $j \to j+1$.

Step 4.

Case 1. $\underset{\sim}{x}_{ss}(t)$ is periodic with small period T:
Solve (3.1) for $\underset{\sim}{x}(t)$ with $\underset{\sim}{x}_0^*(B)$ as initial state from t = 0 to t = T. Calculate

$$\varepsilon_j = x_j(0,\underset{\sim}{x}_0^*(B)) - x_j(T;\underset{\sim}{x}_0^*(B)), \quad j = 1,2,\ldots,n.$$

Case 2. $\underset{\sim}{x}_{ss}(t)$ is not periodic or is periodic with large T:
Solve (3.1) for $\underset{\sim}{x}(t)$ with $\underset{\sim}{x}_0^*(B)$ as initial state from t = 0 to $t = 2(B+2)T_1$. Calculate $_{B+1}\varepsilon_{B+2}$ as defined in (3.27). If

$$\max\{\varepsilon_1,\varepsilon_2,\ldots,\varepsilon_n\} > \varepsilon_0 \qquad \text{(case 1)}$$

$$_{B+1}\varepsilon_{B+2} > \varepsilon_0 \qquad \text{(case 2)}$$

where ε_0 is a sufficiently small positive number, increase B and repeat Steps 0-4.

Step 5. Stop.

F. Illustrative Examples

Example 1. Duffing's Equation with 2 frequency inputs:

We have used the preceding algorithm to solve (2.64) when f(t) contains only 2 input frequencies. The results corresponding to 3 different combinations of parameter k, c_1, c_2, and f(t) are summarized in Table 5 for B = 9, 11, 13, and 17 respectively.

Table 5. Examples Applying the Two-Frequency Algorithm

B	(1) f(t)=0.5 cost +0.5 cos 0.81t		(2) f(t)=0.3 cost +1.5 cos 0.115t		(3) f(t)=(1+cos 0.115t) cost	
	$x_{0_1}^*(B)$	$x_{0_2}^*(B)$	$x_{0_1}^*(B)$	$x_{0_2}^*(B)$	$x_{0_1}^*(B)$	$x_{0_2}^*(B)$
9	1.04898	0.26642	1.27285	0.27251	1.36899	-0.34537
11	1.11403	0.64204	1.24281	0.17135	1.39967	0.00736
13	1.12986	0.63906	1.22548	0.30906	1.34835	0.16875
15	1.11865	0.63562	1.21332	0.33872	1.35403	0.15168
	$_{16}\varepsilon_{17}=0.0021$		$_{16}\varepsilon_{17}=0.0083$		$_{14}\varepsilon_{15}=0.023$	

In each case, an error estimate using (3.27) is calculated and the results are also listed in Table 5. For example, in case 1, we have

$$16\varepsilon_{17} = \|g_{32}(0)\| + \|g_{34}(0)\|$$

$$\triangleq |g_{32,1}(0)| + |g_{32,2}(0)| + |g_{34,1}(0)| + |g_{34,2}(0)|$$

$$= 0.000853 + 0.000444 + 0.000244 + 0.000554 \cong 0.0021 \qquad (3.28)$$

The rate of convergence for these 3 cases are shown in Fig. 5. The convergence rate for case 3 is not as good as the cases 1 and 2 because we have deliberately chosen a poorer initial guess for constrast.

The steady-state waveforms corresponding to the 3 cases listed in Table 5 are shown in Figs. 6(a), 7(a), and 8(a), respectively. The corresponding frequency spectrum calculated by the FFT algorithm [17] are shown in Figs. 6(b), 7(b), and 8(b), respectively.† For all cases, the higher-order harmonic and with modulation components are negligible, as is typical in many practical examples.

Example 2. Transistor Modulator Circuit:

Consider the differential-pair amplitude modulator circuit shown in Fig. 9(a), where $e_1(t)$ and $e_2(t)$ denotes the carrier and signal input, respectively. Using the algorithm described in Appendix A, and the Ebers-Moll circuit model [3] shown in Fig. 9(b) for the transistors, we obtain the following system of 4 implicit differential-algebraic equations for this circuit:

$$-C\frac{dv_1}{dt} - \frac{v_1}{R_L} - i_2 - I_s[e^{\lambda(v_1-V_{cc})}-1] + \alpha I_s[e^{\lambda v_4}-1] = 0$$

$$-I_s[e^{\lambda(v_4+e_1)}-1] + \alpha I_s[e^{\lambda(e_1-V_{cc})}-1] - I_s[e^{\lambda v_4}-1] + \alpha I_s[e^{\lambda(v_1-v_{cc})}-1]$$

$$- I_s[e^{\lambda(v_4+e_2-V_E)}-1] + \alpha I_s[e^{\lambda v_3}-1] = 0 \qquad (3.28)$$

$$-I_s[e^{\lambda v_3}-1] + \alpha I_s[e^{\lambda(v_4+e_2-V_E)}-1] + \frac{1}{R_B}[V_{cc}-V_E+e_2-v_3] = 0$$

$$-L\frac{di_2}{dt} - v_1 = 0$$

Note that the first 3 equations in (3.28) correspond to KCL applied at nodes ①, ②, and ③ respectively, whereas the 4th equation corresponds to KVL applied around the loop formed by the inductor L.

†Note that unlike in the Multi-Frequency Algorithm, the generalized Fourier coefficients are not directly available in this algorithm.

Setting $e_1(t)$ and $e_2(t)$ to zero, we first solve (3.28) for the following dc operating point:

$$v_{1_Q} = 0,\ i_{2_Q} = 0.155 \times 10^{-3},\ v_{3_Q} = 0.259,\ v_{4_Q} = 0.241 \tag{3.29}$$

We then choose $x_1(0) \triangleq v_1(0) = v_{1_Q}$ and $x_2(0) \triangleq i_2(0) = i_{2_Q}$ as our initial guess $\underset{\sim}{x}_0^{(0)}$ and apply the *two-frequency algorithm* for 2 different amplitudes V_2 for the signal $e_2(t)$; namely $V_2 = 4.0$ and 5.3, respectively. For $V_2 = 4.0$, we choose $B = 6$. However, for $V_2 = 5.3$, we choose $B = 13$ to account for the additional harmonics that are likely to be significant in view of the larger input signal amplitude. In both cases, our algorithm converges in 2 iterations and the results are summarized in Table 6.

Table 6. Results obtained with two-frequency algorithm using a 4th order BDF method [3] with a step size $h = 4\pi(10^{-8})$ sec.

case			Initial State		Error Estimate	
			$v_1(0)$	$i_2(0)$	$B+1\varepsilon_{B+2}$ for v_1	$B+1\varepsilon_{B+2}$ for i_2
(1)	V_2=4.0	B=6	-3.927	$0.2387(10^{-3})$	$0.78(10^{-3})$	$0.59(10^{-7})$
(2)	V_2=5.3	B=13	-3.422	$0.1138(10^{-3})$	$0.23(10^{-1})$	$0.95(10^{-5})$

Using the 2 initial states in Table 6, the steady-state waveforms corresponding to the modulator output voltage $v_0(t)$ and the base-to-emitter-voltages $V_{EB}(t)$ for transistors T_1 and T_3 are shown in Figs. 10(a),(b),(c) and 11(a),(b),(c), respectively. Note that the modulator output waveform in Fig. 10(a) is typical of those composed of a carrier and 2 side band frequencies $\omega_1 \pm \omega_2$. Even the waveforms $V_{EB}(t)$ in Figs. 10(b) and (c) are quite smooth, indicating the absence of significant higher-order frequency components. Consequently, very accurate results were obtained with only a relatively small $B = 6$.

On the other hand, the corresponding waveforms for case 2 in Fig. 11 indicate the presence of many more frequency components. Consequently, a much larger B will be needed to obtain results of acceptable accuracy. We found $B = 13$ is adequate for this purpose.

The normalized frequency spectrum corresponding to the output waveforms $v_0(t)$ in case 2 as obtained by the FFT method [17] is shown in Fig. 12.

IV. Concluding Remarks

Two efficient algorithms have been presented for finding almost periodic steady-state response of nonlinear circuits and systems.

The multi-frequency algorithm is very general as it allows any number of commensurable or incommensurable input frequencies $\omega_1, \omega_2, \ldots, \omega_p$. Although the output normally includes only harmonic and inter-modulation frequency components of the form $\nu_k = m_{1k}\omega_1 + m_{2k}\omega_2 + \ldots + m_{pk}\omega_p$, where m_{jk} are integers, other frequency components, such as subharmonics, may also be included in this algorithm if their presence are suspected.

The two-frequency algorithm is applicable only if there are no more than 2 input frequencies. This restriction, however, is more than compensated by its greatly increased computational efficiency, specially when the steady-state response contains many frequency components. That this algorithm is significantly better than algorithm 1 (when applied in the 2-frequency case) is best seen by comparing the number of respective coefficients in Table 4. Note that for B=10, Algorithm 1 must calculate 221 coefficients whereas Algorithm 2 needs to calculate only 21. Note that 2B + 1 increases only by 2 as we increase B by 1; consequently, the two-frequency algorithm remains computationally quite efficient even with a larger B, thereby allowing stronger nonlinearities. This is particularly useful when the amplitude of the higher-frequency input (ω_1) is much larger than that of ω_2, as is common in communication circuits where ω_1 denotes the carrier frequency and ω_2 denotes the signal frequency. In this case, the number of significant harmonic components of ω_2 will be relatively small so that a small B suffices.

It is also interesting to note that in the limiting case where we have only one frequency input (P=1), then (3.5) reduces to $\underset{\sim}{x}_{ss}(t) = g_0(t)$. In this case, the two-frequency algorithm reduces to the usual shooting method [3,11].

Certain numerical ill-conditioning could occur in the Algorithm 1 when the step size Δt is chosen to be too small. The ill-conditioning problem is due to loss of number of significant digits and therfore depends strongly on the choice of the computer.

Finally we remark that if the steady state-solution is not periodic so that the brute-force method is impractical (since we must in theory integrate for all $t \geq 0$), or if the nonlinearity is not sufficiently weak for the Perturbation and Volterra series methods to converge, then our algorithms are presently the only methods available for finding steady-state solutions, let alone their good computational efficiency.

Acknowlegement

The authors would like to thank Mr. E. Nishiyama for programing Example 2 in Section III.

V. Appendix

Appendix A. Explicit Formula for Reduced System of Implicit Equations

Let N be a nonlinear network containing voltage or current-controlled 2-terminal resistors, voltage-controlled 2-terminal capacitors, current-controlled 2-terminal inductors, as well as independent and controlled sources. Mutual couplings are allowed so long as they are restricted to elements belonging to the same class. Let each independent source be considered as part of a "composite" branch as in [3]. Adoping the notations in Section 17-2 of [3], we obtain the following tableau equation for N:

$$\begin{matrix} \text{n-1 KCL equations} \\ \text{b KVL equations} \\ \text{b elements consitutive relations} \end{matrix} \left\{ \begin{matrix} \\ \\ \end{matrix} \right. \begin{bmatrix} \underset{\sim}{A} & \underset{\sim}{0} & \underset{\sim}{0} \\ \underset{\sim}{0} & \underset{\sim}{1} & -\underset{\sim}{A}^T \\ \underset{\sim}{K}_i & \underset{\sim}{K}_v & \underset{\sim}{0} \end{bmatrix} \begin{bmatrix} \underset{\sim}{i} \\ \underset{\sim}{v} \\ \underset{\sim}{v}_n \end{bmatrix} - \begin{bmatrix} \underset{\sim\sim}{AJ} \\ \underset{\sim}{E} \\ \underset{\sim}{g}(\dot{\underset{\sim}{v}}_C, \underset{\sim}{i}_L, \underset{\sim}{v}, \underset{\sim}{i}) \end{bmatrix} = \begin{bmatrix} \underset{\sim}{0} \\ \underset{\sim}{0} \\ 0 \end{bmatrix} \qquad \text{(A-1)}$$

Equation (A-1) consists of a system of (n-1) + 2b implicit equations of the form (1.1) where "b" denotes the number of composite branches and "n" denotes the number of nodes. Our goal in this section is to derive an equivalent system of implicit equations containing fewer number of equations and variables for an important subclass of networks.

In particular, we assume that N contains no loops of capacitors and independent voltage sources, no cut sets of inductors and independent current sources and that all controlled sources are current sources depending on either resistor or capacitor voltages. Consequently, there always exists a normal tree T containing all capacitors and no inductors [3].

If we let $\underset{\sim}{i}_2$ and $\underset{\sim}{v}_2$ denote the current and voltage vectors of all inductors in N, and let $\underset{\sim}{i}_1$ and $\underset{\sim}{v}_1$ denote the current and voltage vectors of the remaining elements, then (A-1) can be recast as follows:

$$\left[\begin{array}{cc|c|cc|c} \underset{\sim}{1} & \underset{\sim}{0} & -\underset{\sim}{Y}_b & \underset{\sim}{0} & \underset{\sim}{0} & \underset{\sim}{0} \\ \underset{\sim}{0} & \underset{\sim}{0} & \underset{\sim}{0} & \underset{\sim}{1} & \underset{\sim}{0} & \underset{\sim}{0} \\ \hline \underset{\sim}{0} & \underset{\sim}{0} & \underset{\sim}{1} & \underset{\sim}{0} & -\underset{\sim}{A}_1^T & \underset{\sim}{0} \\ \underset{\sim}{0} & \underset{\sim}{0} & \underset{\sim}{0} & \underset{\sim}{1} & -\underset{\sim}{A}_2^T & \underset{\sim}{0} \\ \hline \underset{\sim}{A}_1 & \underset{\sim}{A}_2 & \underset{\sim}{0} & \underset{\sim}{0} & \underset{\sim}{0} & \underset{\sim}{0} \end{array}\right] \left[\begin{array}{c} \underset{\sim}{i}_1 \\ \underset{\sim}{i}_2 \\ \hline \underset{\sim}{v}_1 \\ \underset{\sim}{v}_2 \\ \hline \underset{\sim}{v}_n \end{array}\right] - \left[\begin{array}{c} \underset{\sim}{g}(\dot{\underset{\sim}{v}}_c, \underset{\sim}{v}) \\ \underset{\sim}{L}(\underset{\sim}{i}_2)\dot{\underset{\sim}{i}}_2 \\ \hline \underset{\sim}{E}_1 \\ \underset{\sim}{E}_2 \\ \hline \underset{\sim\sim}{AJ} \end{array}\right] = \left[\begin{array}{c} \underset{\sim}{0} \\ \underset{\sim}{0} \\ \hline \underset{\sim}{0} \\ \underset{\sim}{0} \\ \hline \underset{\sim}{0} \end{array}\right] \qquad \text{(A-2)}$$

where the reduced incidence matrix $\underset{\sim}{A}$ is similarly partitioned into $\underset{\sim}{A} = [\underset{\sim}{A}_1\ \underset{\sim}{A}_2]$, and where $\underset{\sim}{L}(\underset{\sim}{i}_2)$ denotes the incremental inductance matrix. Substituting

$$\underset{\sim}{i}_1 = \underset{\sim}{Y}_b\underset{\sim}{v}_1 + \underset{\sim}{g}(\dot{\underset{\sim}{v}}_c,\underset{\sim}{v}) = \underset{\sim}{Y}_b(\underset{\sim}{A}_1^T\underset{\sim}{v}_n+\underset{\sim}{E}_1) + \underset{\sim}{g}(\dot{\underset{\sim}{v}}_c,\underset{\sim}{v}) \tag{A-3}$$

into the last equation in (A-2), we obtain the following reduced system of equations:

$$\underset{\sim}{A}_2\underset{\sim}{i}_2 + (\underset{\sim}{A}_1\underset{\sim}{Y}_b\underset{\sim}{A}_1^T)\underset{\sim}{v}_n = -\underset{\sim}{A}_1\underset{\sim}{Y}_b\underset{\sim}{E}_1 - \underset{\sim}{A}_1\underset{\sim}{g}(\dot{\underset{\sim}{v}}_c,\underset{\sim}{v}) + \underset{\sim}{A}\underset{\sim}{J} \tag{A-4}$$

$$\underset{\sim}{v}_2 = \underset{\sim}{A}_2^T\underset{\sim}{v}_n + \underset{\sim}{E}_2 = \underset{\sim}{L}(i_2)\dot{\underset{\sim}{i}}_2 \tag{A-5}$$

Let $\underset{\sim}{v}_T$ denote the branch voltage vector associated with the normal tree T, and let $\underset{\sim}{v}_L$ denote the corresponding cotree voltages. Since all capacitors are assigned in T, $\underset{\sim}{v}_C$ is a subvector of $\underset{\sim}{v}_T$. Similarly, since all inductors are assigned in the cotree, $\underset{\sim}{v}_2$ is a subvector of $\underset{\sim}{v}_L$. Let the reduced incidence matrix $\underset{\sim}{A}$ be partitioned accordingly into $\underset{\sim}{A}_T$ and $\underset{\sim}{A}_L$, so that KVL assumes the form

$$\underset{\sim}{v} \triangleq \begin{bmatrix} \underset{\sim}{v}_T \\ \hline \underset{\sim}{v}_L \end{bmatrix} = \begin{bmatrix} \underset{\sim}{A}_T \\ \hline \underset{\sim}{A}_L \end{bmatrix}^T \underset{\sim}{v}_n + \begin{bmatrix} \underset{\sim}{E}_T \\ \hline \underset{\sim}{E}_L \end{bmatrix} \tag{A-6}$$

Since the columns of $\underset{\sim}{A}_T$ correspond to tree branches, $\underset{\sim}{A}_T$ is non-singular [3]. Hence we can solve for the node-to-datum voltage vector $\underset{\sim}{v}_n$ from (A-6) to obtain

$$v_n = [\underset{\sim}{A}_T^T]^{-1}[\underset{\sim}{v}_T - \underset{\sim}{E}_T] \tag{A-7}$$

$$\underset{\sim}{v}_L = \underset{\sim}{A}_L^T[\underset{\sim}{A}_T^T]^{-1}[\underset{\sim}{v}_T - \underset{\sim}{E}_T] + \underset{\sim}{E}_L \tag{A-8}$$

Substituting (A-7) and (A-8) into (A-4) and (A-5), and denoting the inductor current vector $\underset{\sim}{i}_2$ by $\underset{\sim}{i}_L$, we obtain

$$\boxed{\underset{\sim}{A}_2\underset{\sim}{i}_L + (\underset{\sim}{A}_1\underset{\sim}{Y}_b\underset{\sim}{A}_1^T)[\underset{\sim}{A}_T^T]^{-1}(\underset{\sim}{v}_T - \underset{\sim}{E}_T) + \underset{\sim}{A}_1\underset{\sim}{Y}_b\underset{\sim}{E}_1 + \underset{\sim}{A}_1\hat{\underset{\sim}{g}}(\dot{\underset{\sim}{v}}_c,\underset{\sim}{v}_T) - \underset{\sim}{A}\underset{\sim}{J} = \underset{\sim}{0}} \tag{A-9}$$

$$\boxed{\underset{\sim}{A}_2^T[\underset{\sim}{A}_T^T]^{-1}(\underset{\sim}{v}_T - \underset{\sim}{E}_T) + \underset{\sim}{E}_2 - \underset{\sim}{L}(i_L)\dot{\underset{\sim}{i}}_L = \underset{\sim}{0}} \tag{A-10}$$

where

$$\hat{\underset{\sim}{g}}(\dot{\underset{\sim}{v}}_c,\underset{\sim}{v}_T) \triangleq \underset{\sim}{g}(\dot{\underset{\sim}{v}}_c,\underset{\sim}{v})\Big|_{\underset{\sim}{v} = [\underset{\sim}{v}_T\ \underset{\sim}{v}_L]^T}$$

and $\underset{\sim}{v}_T$ is given by (A-8),

Equations (A-9)-(A-10) constitute a reduced system of implicit equations in terms of the state variables $\underset{\sim}{x} \triangleq [\underset{\sim}{v}_C\underset{\sim}{i}_L]^T$ and the non-state variables contained within $\underset{\sim}{v}_T$.

Equation (A-9) can be interpreted as the nodal equation of N with all inductor currents i_{L_j} considered as independent sources, and with all node-to-datum voltages expressed in terms of the normal tree voltage vector $\underset{\sim}{v}_T$. Similarly, (A-10) can be interpreted as the fundamental loop equations (relative to the normal tree T) formed by the inductor links. These interpretations allow us to write down the reduced system of implicit equations of simple nonlinear networks -- such as that considered in section III -- by inspection. If N contains loops of capacitors and independent voltage sources, or cut sets of inductors and independent current sources, the above procedure can be easily generalized by first expressing the cotree capacitor voltages in terms of tree capacitor voltages, and tree inductor currents in terms of cotree inductor currents [3].

APPENDIX B

The matrix $\underset{\sim}{\Gamma}^T\underset{\sim}{\Gamma}$ in Theorem 3 is non singular if, and only if,

$$\Delta t \neq \frac{2n\pi}{|\nu_i \pm \nu_k|}$$

where $\underset{\sim}{\Gamma}$ is a $Z\times(2N+1)$ matrix, where $Z \geq 2N+1$.

Proof. $\underset{\sim}{\Gamma}^T\underset{\sim}{\Gamma}$ is clearly symmetric and positive semi-definite and hence its eigenvalues $\lambda_1, \lambda_2, \ldots, \lambda_n$ are real and non-negative. Hence $\det(\underset{\sim}{\Gamma}^T\underset{\sim}{\Gamma}) = \lambda_1, \lambda_2, \ldots \lambda_n \neq 0 \Leftrightarrow$ all eigenvalues are positive $\Leftrightarrow \underset{\sim}{\Gamma}^T\underset{\sim}{\Gamma}$ is positive definite $\Leftrightarrow \underset{\sim}{x}^T(\underset{\sim}{\Gamma}^T\underset{\sim}{\Gamma})\,\underset{\sim}{x} > 0$ for all $\underset{\sim}{x} \neq \underset{\sim}{0}$

Hence, we have

$\det(\underset{\sim}{\Gamma}^T\underset{\sim}{\Gamma}) \neq 0 \Leftrightarrow$ columns of $\underset{\sim}{\Gamma}$ are linearly independent. (B-2)

The matrix $\underset{\sim}{\Gamma}$ in (2.17) can be recast as follows:

$$\underset{\sim}{\Gamma} = \underbrace{\begin{bmatrix} 1 & 1 & 1 & \cdots & 1 & 1 \\ 1 & e^{j\theta_1} & e^{-j\theta_1} & \cdots & e^{j\theta_N} & e^{-j\theta_N} \\ 1 & e^{j2\theta_1} & e^{-j2\theta_1} & \cdots & e^{j2\theta_N} & e^{-j2\theta_N} \\ \vdots & \vdots & \vdots & & \vdots & \vdots \\ 1 & e^{jZ\theta_1} & e^{-jZ\theta_1} & \cdots & e^{jZ\theta_N} & e^{-jZ\theta_N} \end{bmatrix}}_{\underset{\sim}{\Gamma}'} \underbrace{\begin{bmatrix} 1 & 0 & 0 & \cdots & 0 & 0 \\ 0 & 0.5 & -j0.5 & \cdots & 0 & 0 \\ 0 & 0.5 & j0.5 & \cdots & 0 & 0 \\ \vdots & \vdots & \vdots & \ddots & & \\ 0 & 0 & 0 & & 0.5 & -j0.5 \\ 0 & 0 & 0 & & 0.5 & j0.5 \end{bmatrix}}_{\underset{\sim}{D}} \quad \text{(B-3)}$$

where $\theta_1 \triangleq \nu_i \Delta t$. Since $\underset{\sim}{D}$ is clearly non-singular,

Columns of $\underset{\sim}{\Gamma}$ are linearly independent

$\Leftrightarrow$ Columns of $\underset{\sim}{\Gamma}'$ are linearly independent

$\Leftrightarrow$ $e^{j\theta_i} \neq e^{\pm j\theta_k}$ and $e^{\pm j\theta_i} \neq 1$ for any $i \neq k$

$\Leftrightarrow$ $\theta_i \pm \theta_k \neq \pm 2n\pi$ and $\theta_i \neq \pm 2n\pi$, for any integer n

$\Leftrightarrow$ $\theta_i \pm \theta_k \neq \pm 2n\pi$ for any integer n (B-4)

It follows from (B.2) and (B.4) that

$$\det(\underset{\sim}{\Gamma}^T\underset{\sim}{\Gamma}) \neq 0 \Leftrightarrow \nu_i \Delta t \pm \nu_K \Delta t \neq \pm 2n\pi \Leftrightarrow \Delta t \neq \frac{2n\pi}{|\nu_i \pm \nu_k|}$$

■

APPENDIX C

The matrix $\underset{\sim}{\Omega}(B)$ in (3.9) is <u>non singular</u> if, and only if, there exists an integer L_2 such that

$$\frac{\omega_2}{\omega_1} \neq \frac{L_2}{L_1}, \quad L_1 = 1,2,\ldots,2B \tag{C-1}$$

<u>Proof.</u> We can recast $\underset{\sim}{\Omega}(B)$ in (3.9) as follows:

$$\underset{\sim}{\Omega}(B) = \underbrace{\begin{bmatrix} 1 & 1 & 1 & \cdots & 1 & 1 \\ 1 & e^{j\phi} & e^{-j\phi} & \cdots & e^{jB\phi} & e^{-jB\phi} \\ 1 & e^{j2\phi} & e^{-j2\phi} & \cdots & e^{j2B\phi} & e^{-j2B\phi} \\ \vdots & \vdots & \vdots & \vdots\vdots\vdots & \vdots & \vdots \\ 1 & e^{j2B\phi} & e^{-j2B\phi} & \cdots & e^{j2B^2\phi} & e^{-j2B^2\phi} \end{bmatrix}}_{\underset{\sim}{\Omega}'(B)} \underbrace{\begin{bmatrix} 1 & 0 & 0 & \cdots & 0 & 0 \\ 0 & 0.5 & -j0.5 & \cdots & 0 & 0 \\ 0 & 0.5 & j0.5 & \cdots & 0 & 0 \\ \vdots & \vdots & \vdots & \ddots & & \\ 0 & 0 & 0 & & 0.5 & -j0.5 \\ 0 & 0 & 0 & & 0.5 & j0.5 \end{bmatrix}}_{\underset{\sim}{Q}} \tag{C-2}$$

where $\phi \triangleq \omega_2 T_1$. Since $\underset{\sim}{Q}$ is non-singular,

$\underset{\sim}{\Omega}(B)$ is non-singular

$\Leftrightarrow$ Columns of $\underset{\sim}{\Omega}'(B)$ are linearly independent

$\Leftrightarrow$ $e^{jk\phi} - e^{ji\phi} \neq 0$ for $i,k = 0,\pm 1, \pm 2,\ldots \pm B$, $i \neq k$

$\Leftrightarrow$ $1 - e^{jL_1\phi} \neq 0$ for $L_1 = 1,2,\ldots,2B$

$\Leftrightarrow$ $L_1 \phi \neq 2L_2\pi$ for any integer L_2 (C-3)

Substituting $\phi \triangleq \omega_2 T_1 = 2\pi\omega_2/\omega_1$ into (C-3), we obtain:

$\Omega(B)$ is non-singular

$\Leftrightarrow$ $L_1(\omega_2/\omega_1) \neq L_2$.

■

APPENDIX D

If ω_1 and ω_2 are rational numbers, we can make $\underset{\sim}{\Omega}(B)$ non-singular by choosing

$$B < \frac{T}{2T_1} \tag{D-1}$$

Proof. Let $\omega_1 \triangleq m_1/n_1$ and $\omega_2 \triangleq m_2/n_2$ be irreducible fractions. Then $T_1 = 2\pi(n_1/m_1)$, $T_2 = 2\pi(n_2/m_2)$, and $T = 2\pi(n/m)$, where n = L.C.M. $\{n_1,n_2\}$ and m = G.C.D.$\{m_1,m_2\}$. Hence $m_1 = mm_1'$, $m_2 = mm_2'$, $n_1 = kn_1'$, $n_2 = kn_2'$, and $n = kn_1'n_2'$ for some integer k.

Now, since G.C.D.$\{m_1',m_2'\} = 1$, G.C.D.$\{m_1',n_1'\} = 1$, and G.C.D.$\{m_2',n_2'\} = 1$, we have G.C.D.$\{m_2'n_1', m_1', n_2'\} = 1$. It follows that if

$$\max\{L_1\} = 2B < m_1'n_2' \tag{D-2}$$

then

$$L_1\left(\frac{\omega_2}{\omega_1}\right) = L_1\left(\frac{T_1}{T_2}\right) = L_1\left(\frac{m_2n_1}{m_1n_2}\right) = L_1\left(\frac{m_2'n_1'}{m_1'n_2'}\right) \neq \text{integer} \tag{D-3}$$

But (D.2) is equivalent to

$$2BT_1 < m_1'n_2'T_1 = m_1'n_2'(n_1/m_1)(m/n)T = \left(\frac{m_1'm}{m_1}\right)\left(\frac{n_2'n_1}{n}\right)T = \frac{n_2'kn_1'}{kn_1'n_2'}T = T \tag{D-4}$$

Hence, if $2BT_1 < T$, then (C.1) holds. ∎

REFERENCES

1. K. K. Clarke and D. T. Hess, Communication Circuits: Analysis and Design, Addison-Wesley Publishing Company, 1971.

2. Transmission Systems for Communications, Bell Telephone Laboratories, Inc. Revised 4th Edition, 1971.

3. L. O. Chua and P. M. Lin, Computer-Aided Analysis of Electronic Circuits: Algorithms and Computational Techniques, Prentice Hall, 1975.

4. L. O. Chua and D. N. Green, "A qualitative analysis of the behavior of dynamic nonlinear networks: steady state solutions of nonautonomous networks," IEEE Trans. Circuits and Systems, Vol. CAS-23, pp. 530-550, September 1976.

5. L. O. Chua and C. Y. Ng, "Frequency domain analysis of nonlinear systems: general theory," IEE J. Electronic Circuits and Systems, Vol. 3, pp. 165-185, 1979.

6. Y. L. Kuo,"Distortion analysis of bipolar transistor circuits," IEEE Trans. Circuit Theory, Vol. CT-20, pp. 709-716, November 1973.

7. J. J. Bussgang, L. Ehrman, and J. W. Graham, "Analysis of nonlinear systems with multiple inputs," Proc. IEEE, Vol. 62, No. 8, pp. 1088-1119, August 1974.

8. T. B. M. Neil, "Improved method of analyzing nonlinear electrical networks." Electronic Letters, Vol. 5, No. 1, pp. 13-15, January 1969.

9. M. Urabe, "On the existence of quasiperiodic solutions to nonlinear quasiperiodic differential equations." Nonlinear Vibration Problems, Warsaw, pp. 85-93, 1974.

10. T. Mitsui, "Investigation of numerical solutions of some nonlinear quasiperiodic differential equations." Publ. of the Research Institute for Mathematical Sciences Kyoto Univ., Vol. 13, No. 3, pp. 793-820, 1977.

11. T. J. Aprille, Jr. and T. N. Trick, "Steady-state analysis of nonlinear circuits with periodic input." Proc. IEEE, Vol. 60, No. 1, pp. 108-114, January 1972.

12. M. S. Nakhla and F. H. Branin, Jr., "Determining the periodic response of nonlinear systems by a gradient method." Circuit Theory and Applications, Vol. 5, pp. 255-273, 1977.

13. J. K. Hale, Ordinary differential equations, J. Wiley, 1969.

14. C. Hayashi, Nonlinear Oscillation in Physical Systems, McGraw-Hill, New York, N.Y., 1964.

15. Y. Ueda, Some Problems on the Theory of Nonlinear Oscillations, Nippon Printing and Publishing Co., Ltd., Osaka, Japan, 1968.

16. Y. Ueda, "Steady motions exhibited by Duffing's equation -- a picture book of regular and chaotic motions," in Conf. on New Approaches to Nonlinear Problems in Dynamics, (Monterey, CA), Dec. 9-14, 1979; to appear in the Engineering Foundation Conference Proc., SIAM.

17. E. O. Brigham, The Fast Fourier Transformation, Prentice Hall, Englewood Cliffs, N.J. 1974.

FIGURE CAPTIONS

Fig. 1 Steady-state waveform for Duffing's equation $\ddot{x} + 0.1\dot{x} + 2x + x^3 = 0.4 \cos t + 0.4 \cos 0.35t + 0.4 \cos 0.155t$.
(a) Solid waveform represents approximate solution obtained with multi-frequency algorithm. Solid dots denote solution obtained by numerical solution of (2.64) starting from $\underset{\sim}{x}_0^* = (0.69667, -0.18304)$ from Case 1.
(b) Discrete frequency spectrum obtained from (2.27).

Fig. 2 Steady-state waveform for Duffing's equation $\ddot{x} + 0.1\dot{x} + 2x + x^3 = 0.4 \cos t + + 0.4 \cos 0.85t + 0.4 \cos 0.17t$.
(a) Solid waveform represents approximate solution obtained with multi-frequency algorithm. Solid dots denote solution obtained by numerical solution of (2.64) starting from $\underset{\sim}{x}_0^* = (0.79298, -0.13834)$ from Case 2.
(b) Discrete frequency spectrum obtained from (2.27).

Fig. 3 The rate of convergence for Case 1 (shown dotted) and Case 2 (shown solid) in the Examples in Table 2. Horizontal axis indicates the iteration number j. Vertical axis indicates the error $\varepsilon^{(j)}$ computed at the jth iteration using (2.67).

Fig. 4 Geometrical interpretation of (3.4) for B = 1,2,...,10. Each solid dot denotes one frequency component $m_{1k}\omega_1 + m_{2k}\omega_2$.

Fig. 5 The rate of convergence for Cases 1, 2, and 3 in the Examples in Table 3. Horizontal axis indicates the iteration number j. Vertical axis indicates the error estimated by

$$\varepsilon^{(j)} = \sqrt{F_1^2(\underset{\sim}{x}_0^{(j)};B) + F_2^2(x_0^{(j)};B)} .$$

Fig. 6 (a) Steady-state waveform for Duffing's equation $\ddot{x} + 0.06\dot{x} + x + x^3 = 0.5 \cos t + 0.5 \cos 0.81\ t$ (Case 1)
(b) Normalized frequency spectrum of (a).

Fig. 7 (a) Steady-state waveform for Duffing's equation $\ddot{x} + 0.05\dot{x} + x + x^3 = 0.3 \cos t + 1.5 \cos 0.115\ t$ (Case 2)

(b) Normalized frequency spectrum of (a).

Fig. 8 (a) Steady-state waveform for Duffing's equation $\ddot{x} + 0.1\dot{x} + x + x^3 = (1 + \cos 0.115\ t) \cos t$ (Case 3)
(b) Normalized frequency spectrum of (a).

Fig. 9 (a) Differential-pair amplitude modulator circuit. $V_{cc} = 10V$, $V_E = 5V$, $L = 2$ mH, $C = 500$ pF, $R_L = 20$ kΩ, $R_B = 15$ kΩ, $e_1(t) = 0.01 \cos 0.115(10^6)t$ and $e_2(t) = V_2 \cos 0.115(10^6)t$.

(b) Ebers-Moll transistor circuit model with the 2 diodes described by $I_{dk} = I_s[e^{\lambda V_{dk}} - 1]$, $I_s = 10^{-8}$A, $\lambda = 40$, $\alpha = 0.99$.

Fig. 10 (a) Steady-state output voltage waveform $v_o(t)$ for Case 1: carrier signal $e_1(t) = 0.1 \cos 10^6\ t$, input signal $e_2(t) = 4.0 \cos 0.115(10^6)t$
(b) Corresponding base-to-emitter voltage waveform $v_{EB}(t)$ for transistor T_1.
(c) Corresponding base-to-emitter voltage waveform $v_{EB}(t)$ for transistor T_3.

Fig. 11 (a) Steady-state output voltage waveform $V_o(t)$ for Case 2: carrier signal $e_1(t) = 0.1 \cos 10^6\ t$, input signal $e_2(t) = 5.3 \cos 0.115(10^6)t$.
(b) Corresponding base-to-emitter voltage waveform $v_{EB}(t)$ for transistor T_1.
(c) Corresponding base-to-emitter voltage waveform $v_{EB}(t)$ for transistor T_3.

Fig. 12 Normalized frequency spectrum for the modulator output voltage waveform in Fig. 11(a) (Case 2)

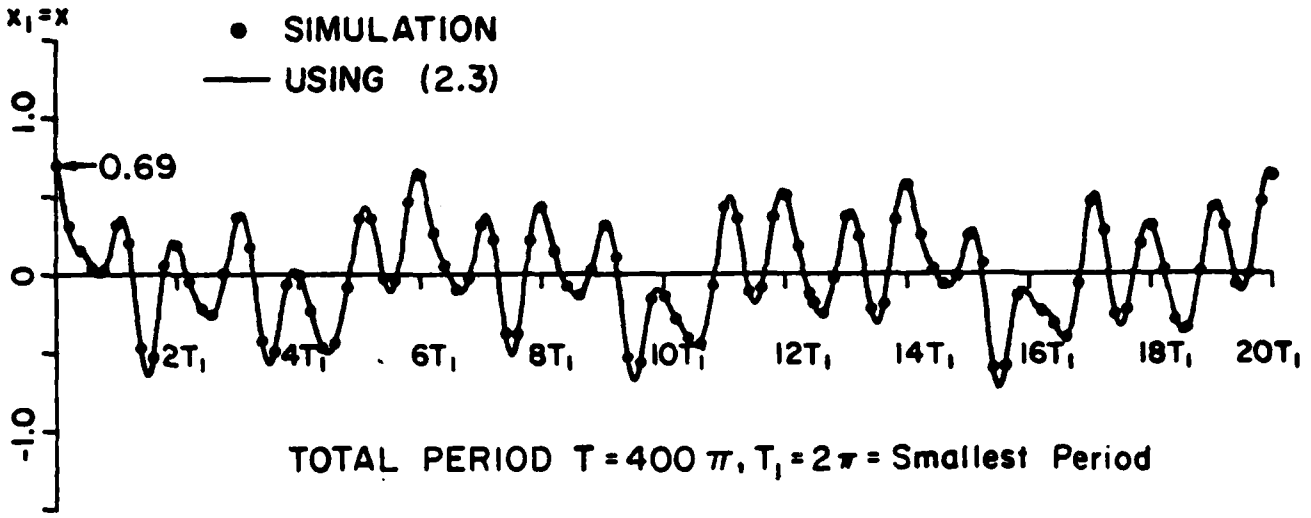

TOTAL PERIOD $T = 400\pi$, $T_1 = 2\pi$ = Smallest Period

(a)

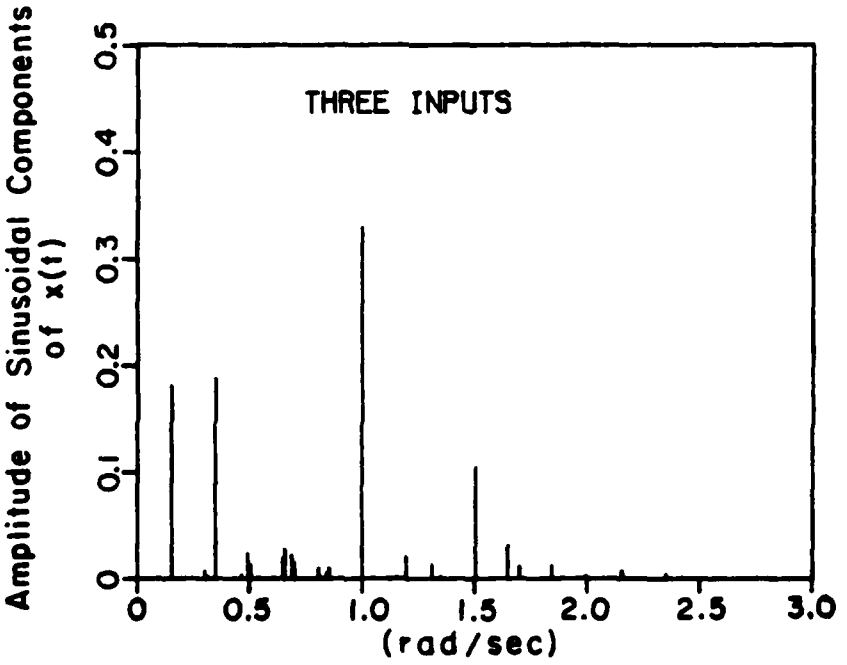

(b)

Fig. 1

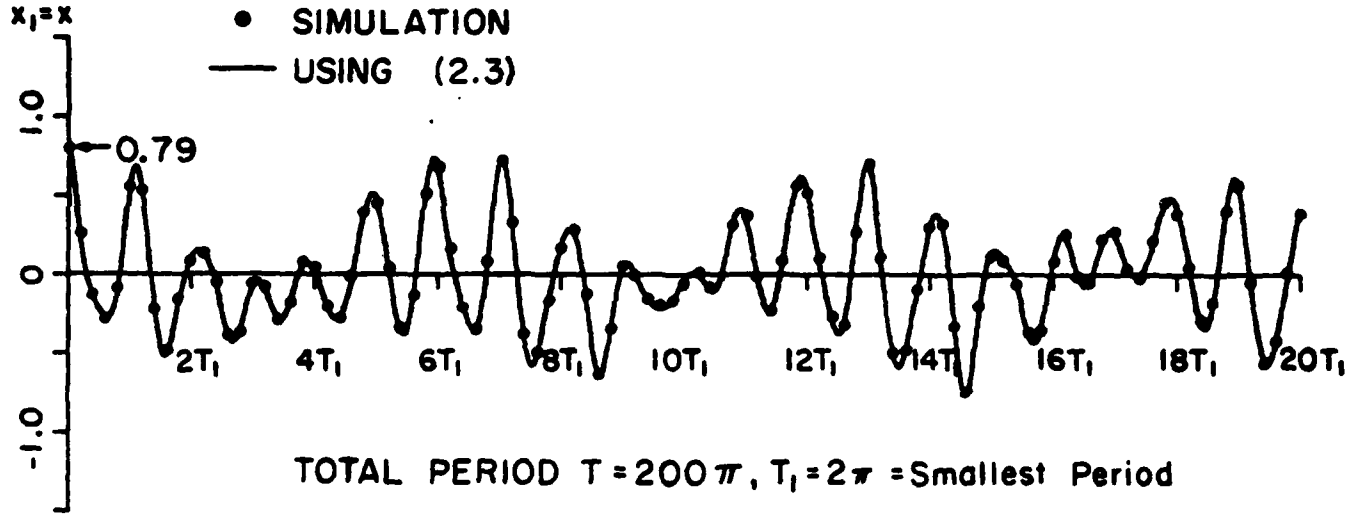

TOTAL PERIOD $T = 200\pi$, $T_1 = 2\pi$ = Smallest Period

(a)

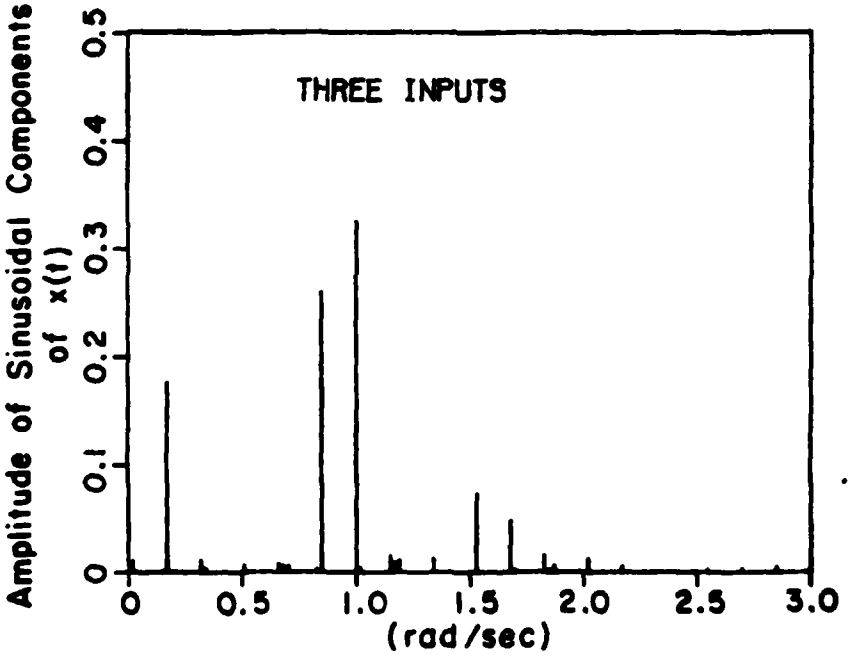

(b)

Fig. 2

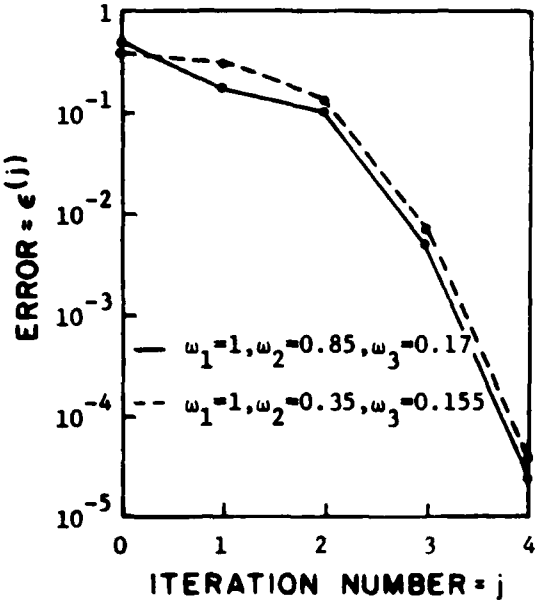

Fig. 3

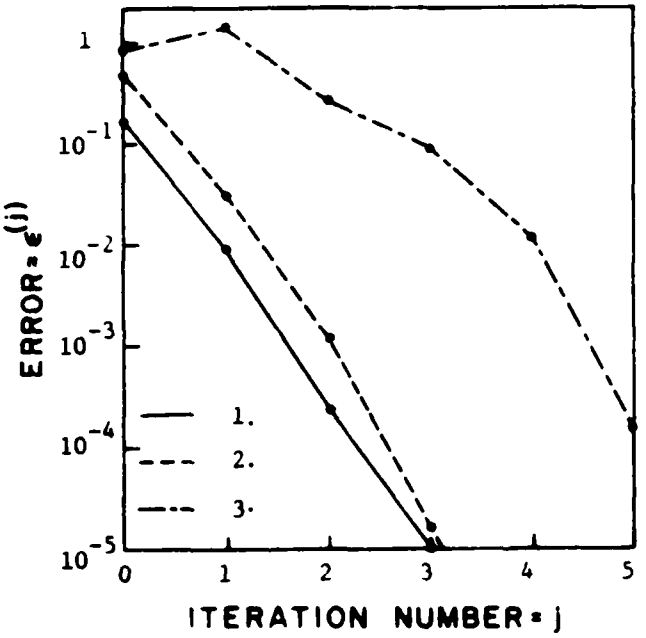

Fig. 5

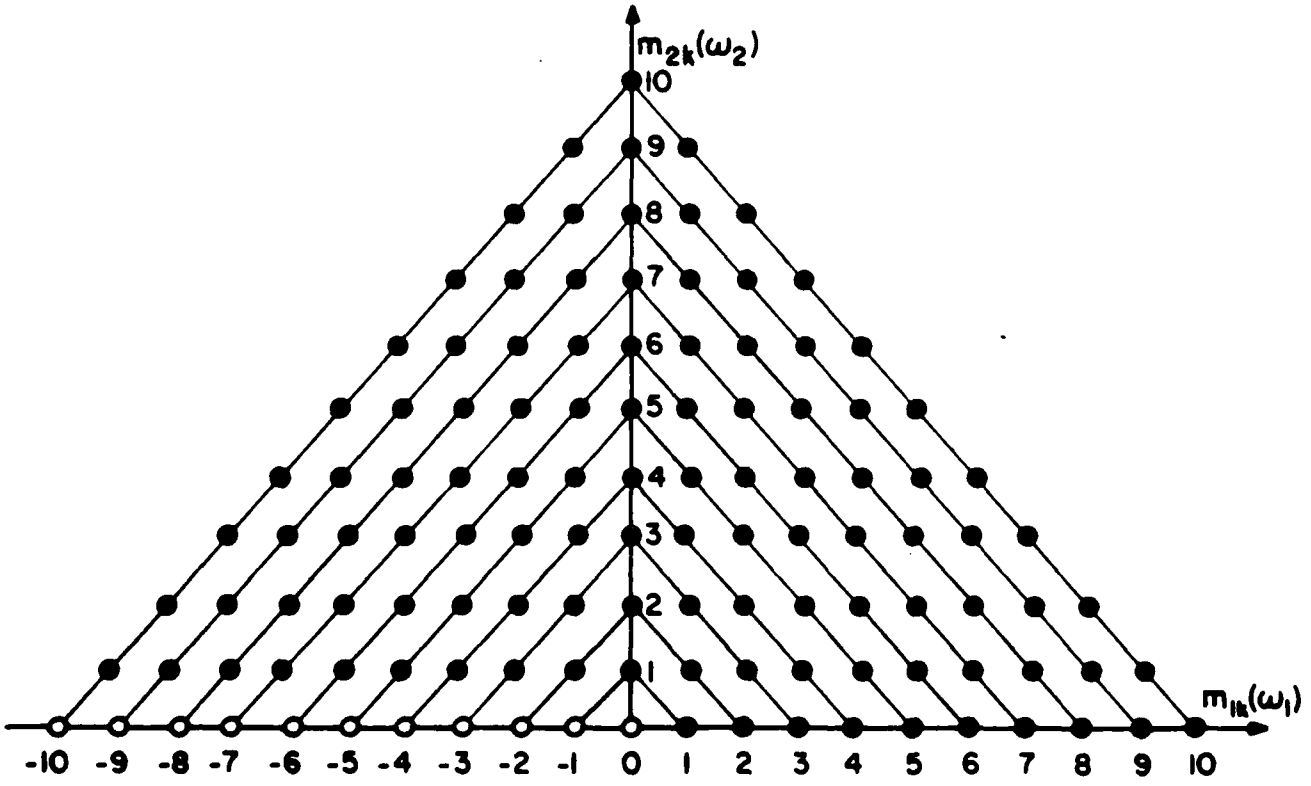

Fig. 4

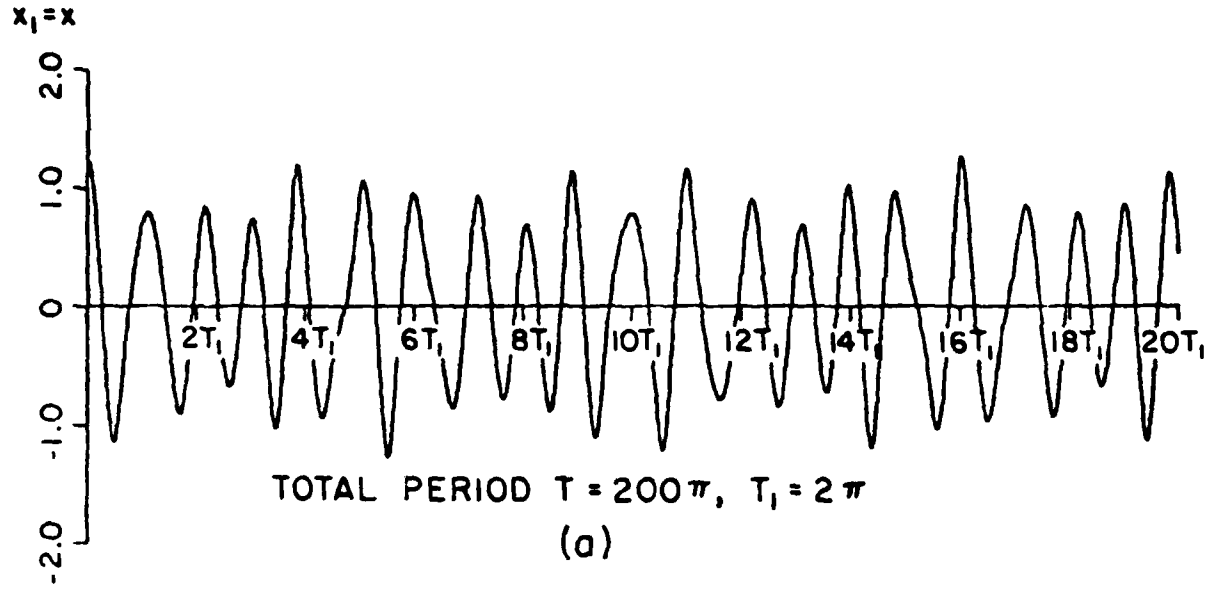

TOTAL PERIOD $T = 200\pi$, $T_1 = 2\pi$

(a)

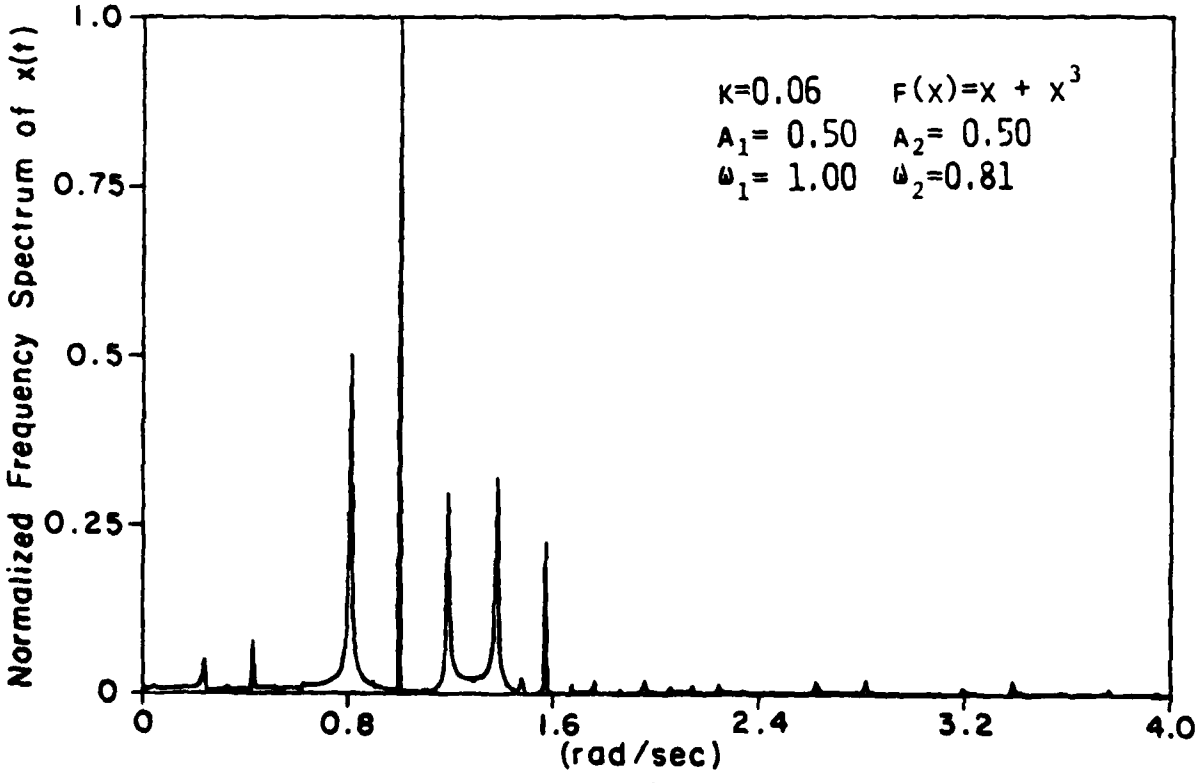

(b)

Fig. 6

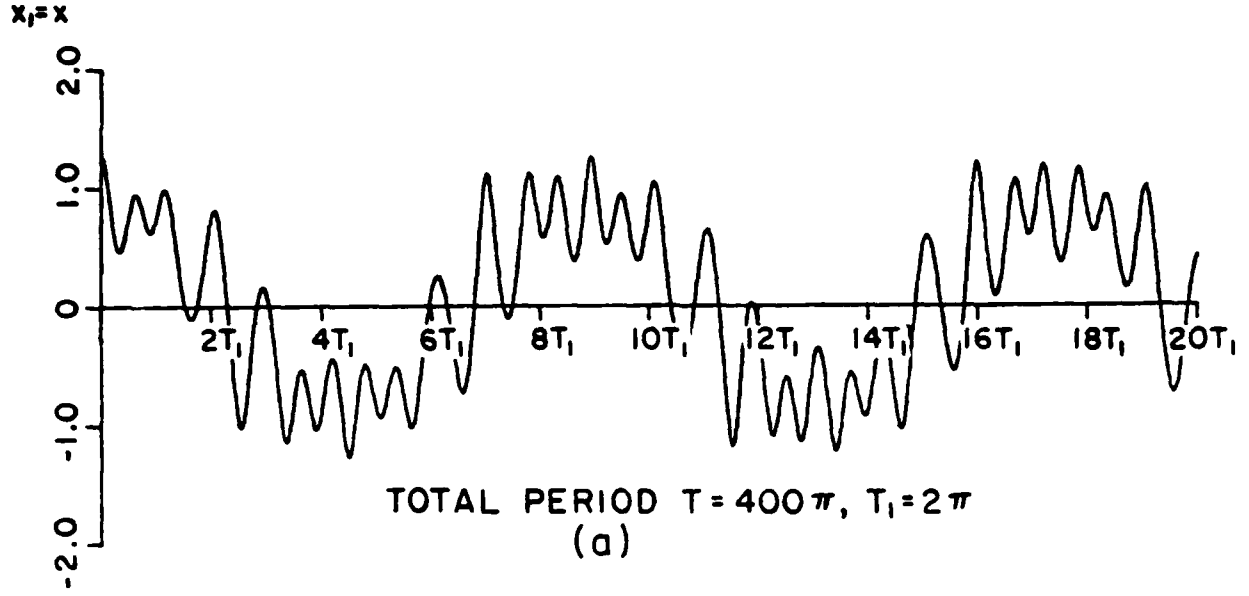

TOTAL PERIOD $T = 400\pi$, $T_1 = 2\pi$

(a)

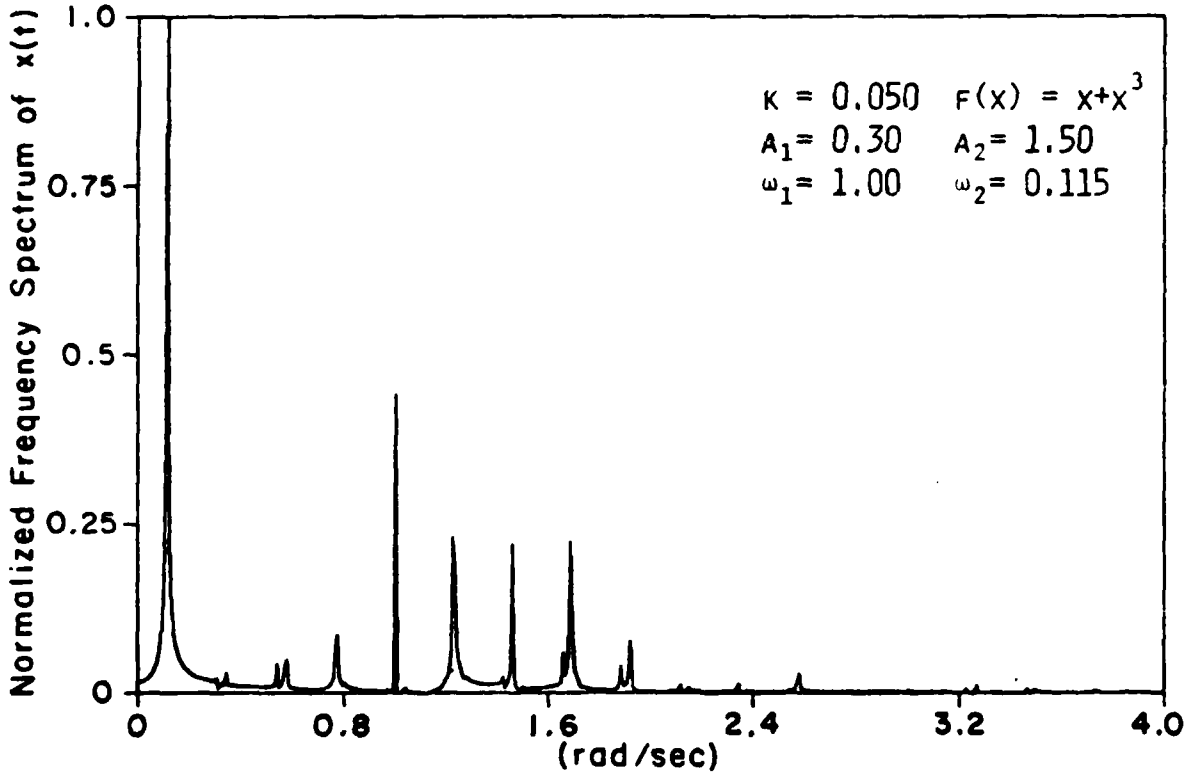

(b)

Fig. 7

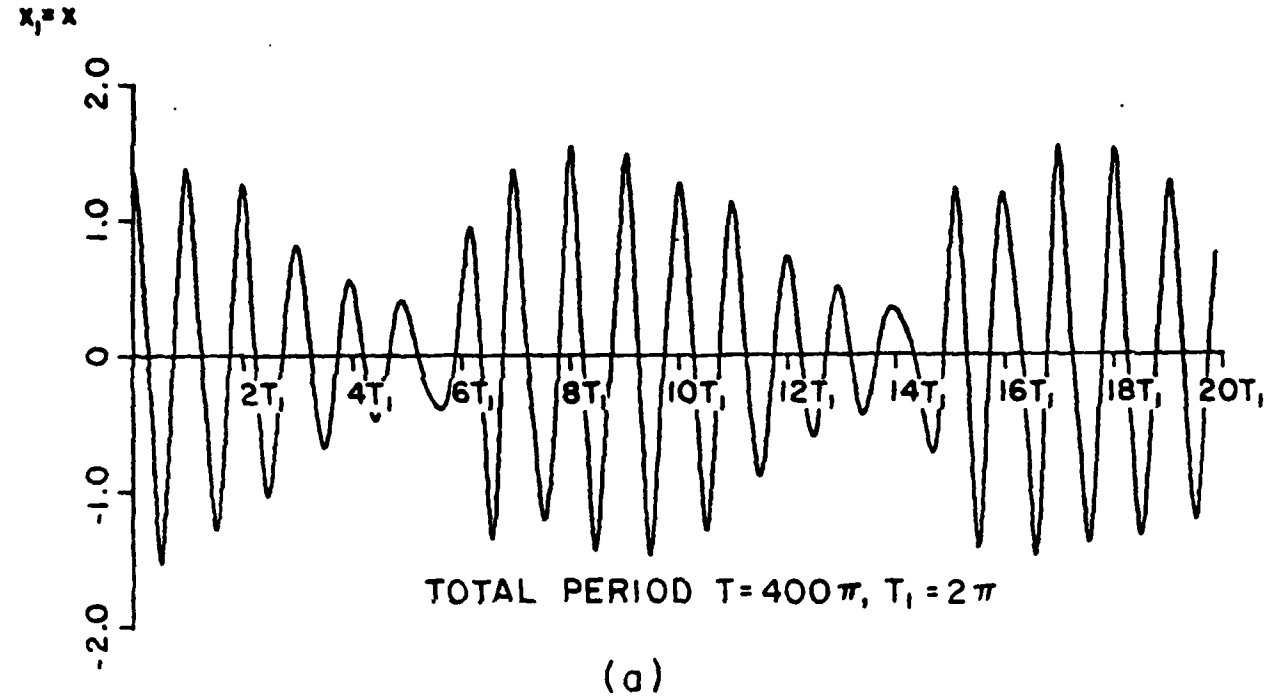
$x_1 = x$
2.0
1.0
0
-1.0
-2.0
2T1
4T1
6T1
8T1
10T1
12T1
14T1
16T1
18T1
20T1
TOTAL PERIOD T=400π, T1=2π

(a)

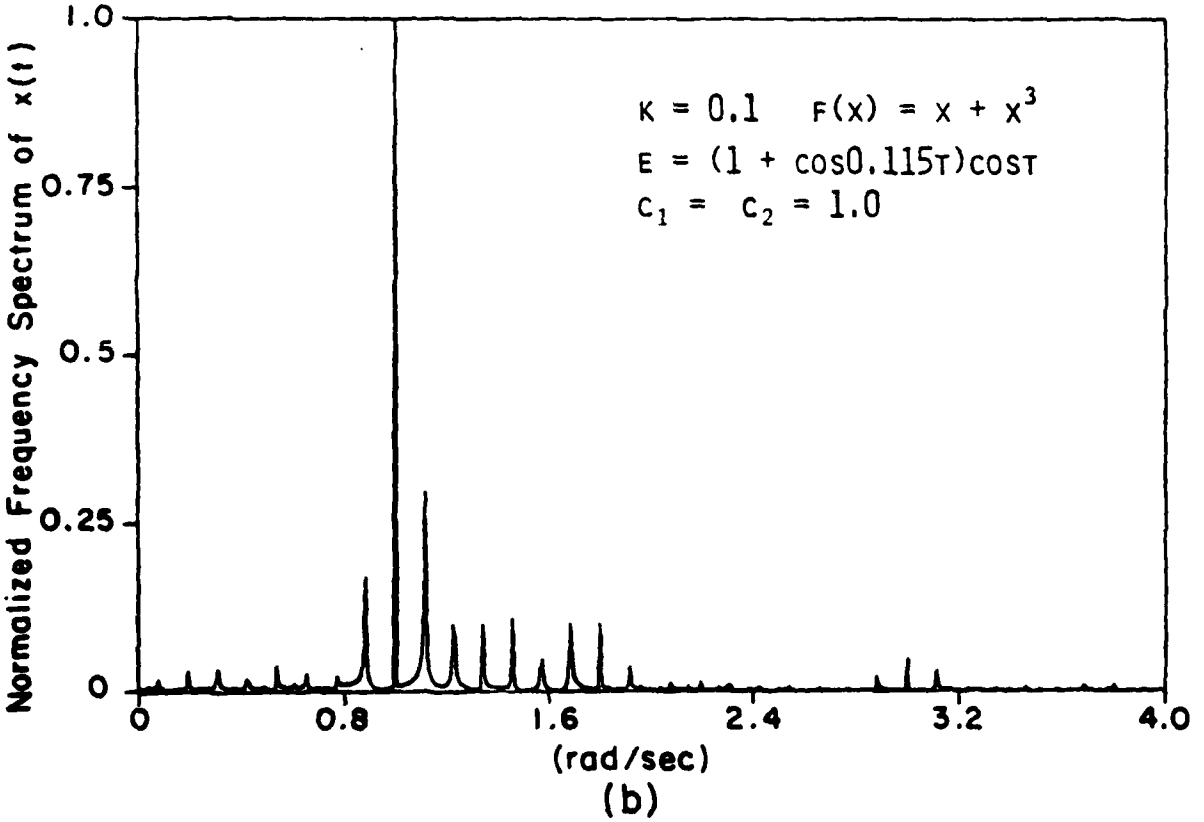
Normalized Frequency Spectrum of x(t)
1.0
0.75
0.5
0.25
0
K = 0.1 F(x) = x + x3
E = (1 + cos0.115T)cosT
C1 = C2 = 1.0
0
0.8
1.6
2.4
3.2
4.0
(rad/sec)

(b)

Fig. 8

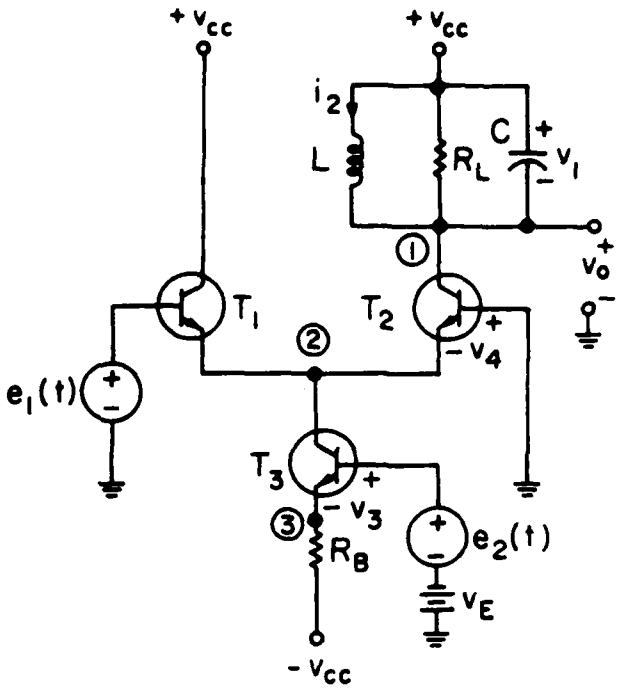
+ Vcc
+ Vcc
i2
L
RL
C
V1
①
Vo
T1
T2
②
e1(t)
- V4
T3
③
- V3
RB
e2(t)
VE
- Vcc

(a)

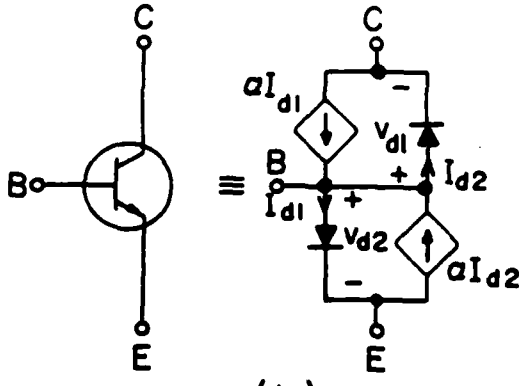
C
B
E
≡
C
aId1
Vd1
B
Id2
Id1
Vd2
aId2
E

(b)

Fig. 9

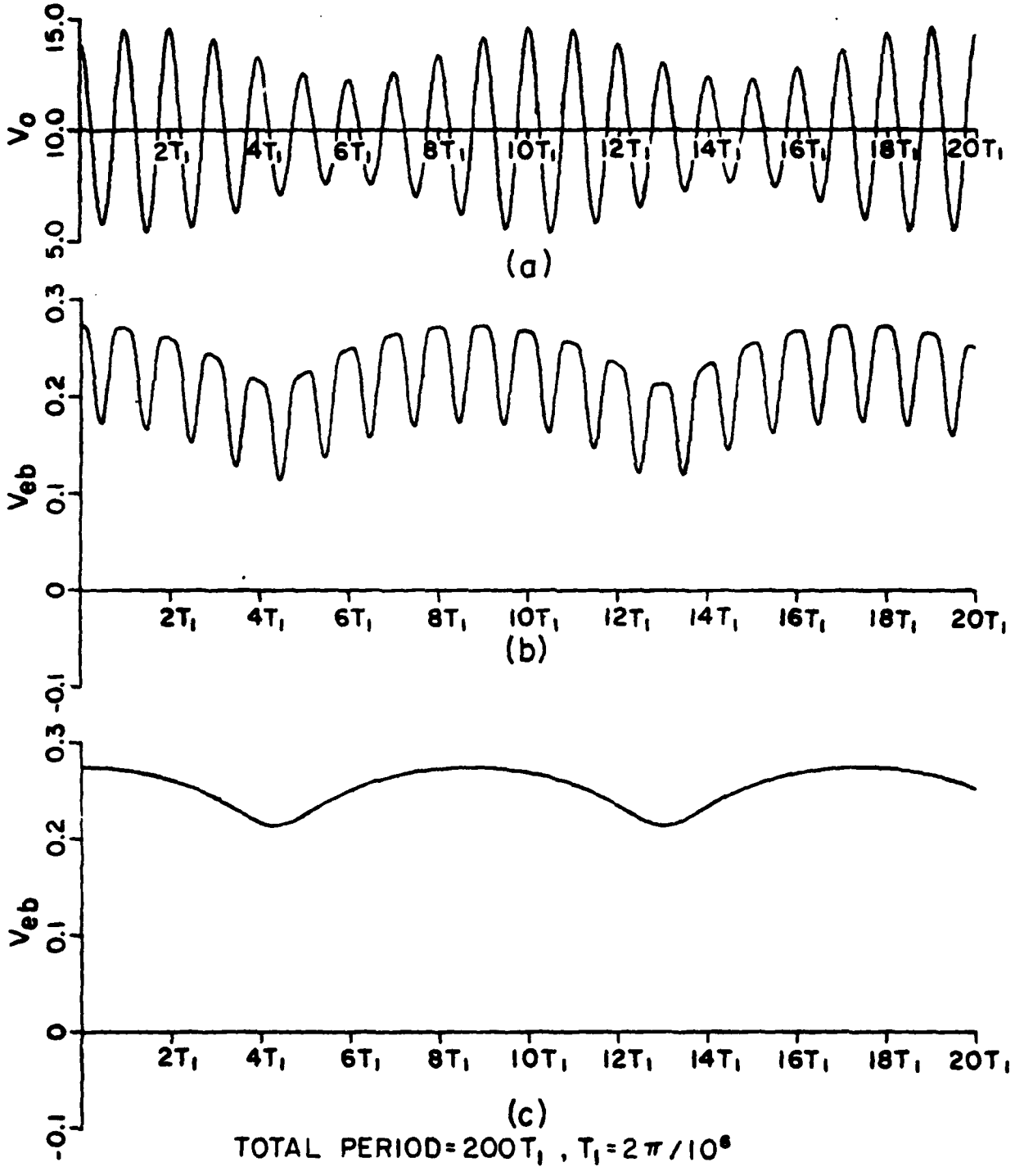

TOTAL PERIOD = $200T_1$, $T_1 = 2\pi/10^6$

Fig. 10

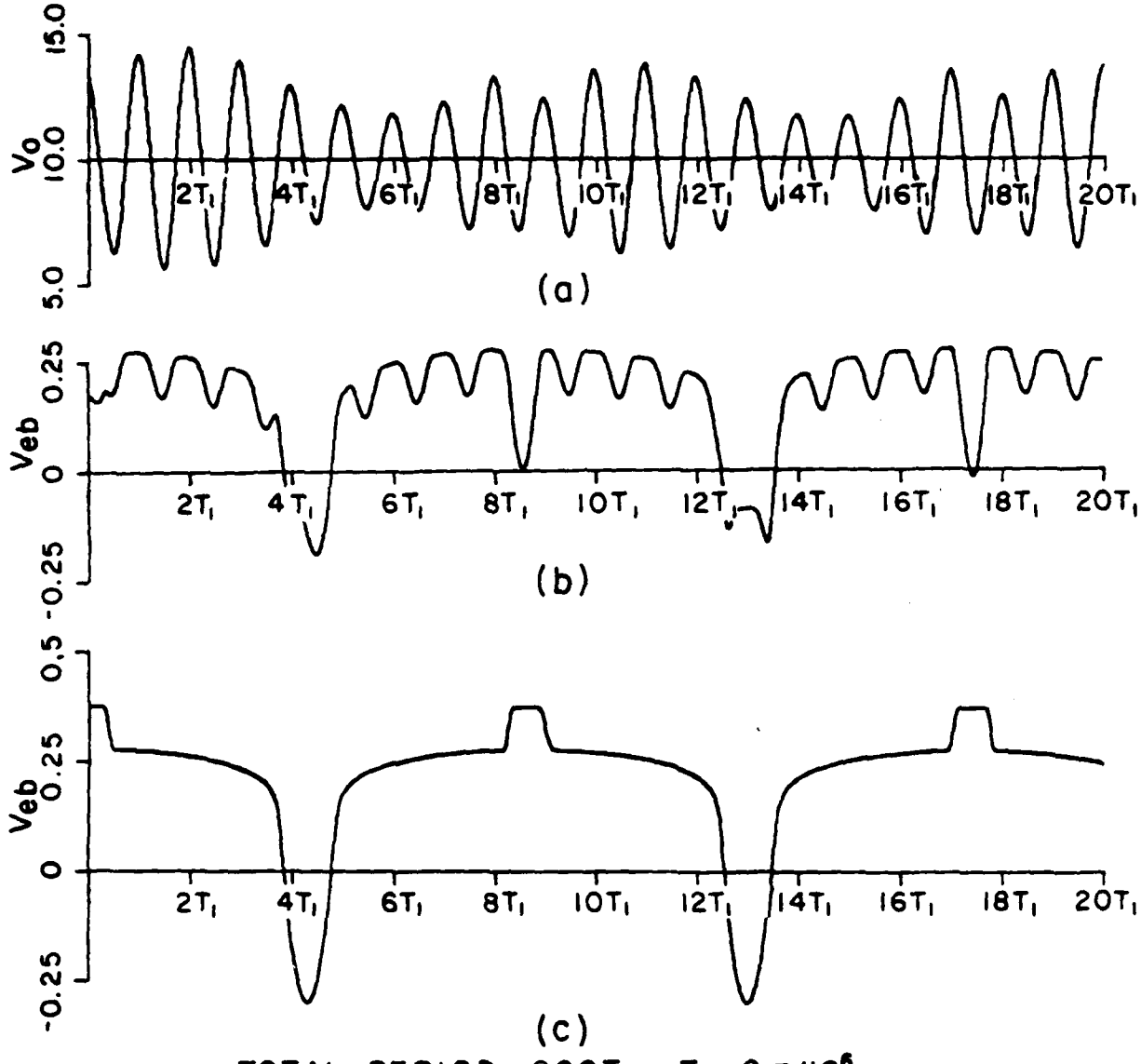

TOTAL PERIOD = $200T_1$, $T_1 = 2\pi/10^6$

Fig. 11

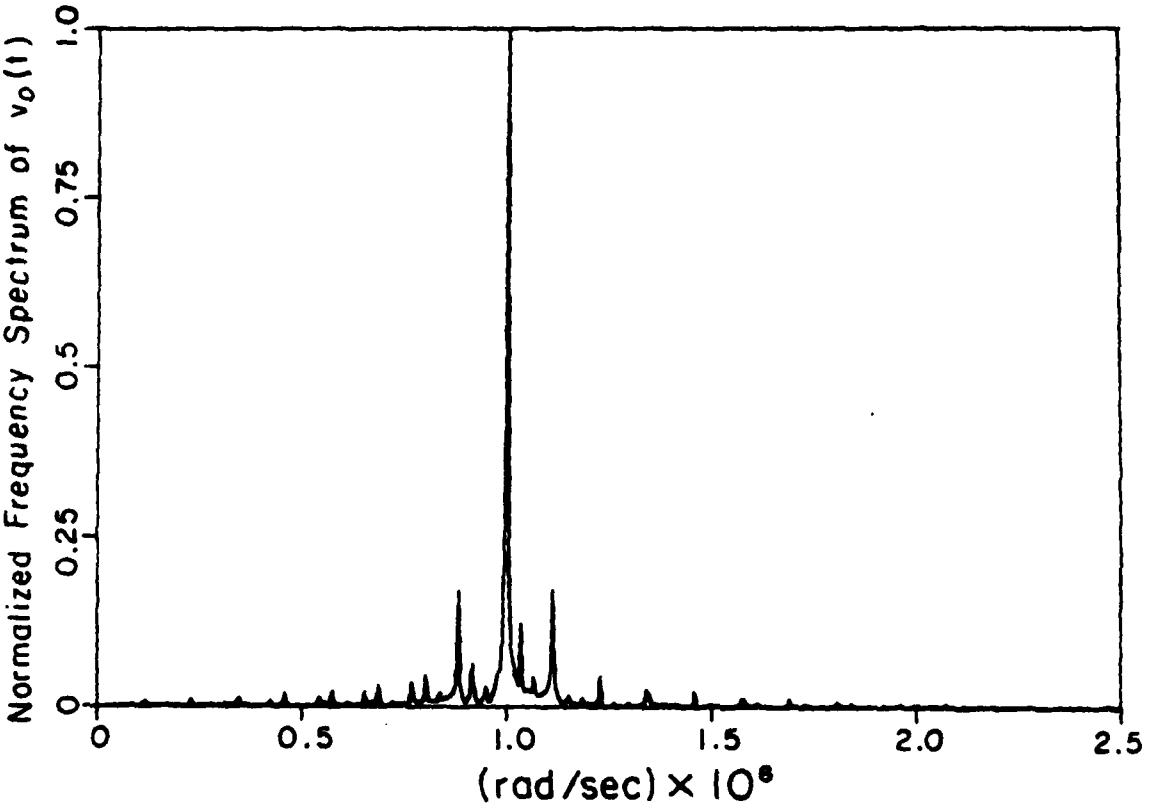
Normalized Frequency Spectrum of $v_0(1)$
0
0.25
0.5
0.75
1.0
0
0.5
1.0
1.5
2.0
2.5
(rad/sec) × 10^6

Fig. 12